C1. A Basis for Stream Channel Classification

C1.1 OVERVIEW

This appendix addresses the basis for classification of the watercourses in southern California, a concept that is necessary to understand their stability and sensitivity to disturbance. The proposed classification system (see Section 4) establishes a context for the application of effective work concepts (dominant discharge) and provides a means for predicting the sensitivity of channels to changes in the driving mechanisms. Appendix C2 examines the concept of dominant discharge based on field investigations in 2004. The morphological relationships that support these concepts are presented in Appendix C3. Channel response in terms of adjustment of the meso-scale features (channel cross-section area) are discussed in Appendix C.4, with Enlargement Curves presented that are based on a comparison of existing cross-section profiles with historic cross-sections spanning several decades.

C1.2 INTRODUCTION

In natural systems, classification schemes are proposed to divide what is essentially a continuum of attributes into discrete groupings. In common with all aspects of earth science, the classification of stream channels is based on both morphology (form) and physical process, with inherent advantages and disadvantages. Classification of channels by form has practical applications to understanding stream behavior in time frames of engineering interest (decades) and the subsequent development of appropriate management programs. The disadvantage of using morphologically-based channel classification methods without reference to process is that the former approach may not be applicable to unstable channel systems. Since urban channels are typically unstable, the proposed classification scheme incorporates aspects of both form and process as follows:

- The organization of channels by fluvial features measured at the micro-, meso-, and macro-scale level. Micro-scale features are those fluvial forms having dimensions of eddies and turbulence in the flow field, e.g. ripples and dunes, micro-pools, the imbricate structures. Meso-scale features are those fluvial forms having dimensions at the scale of the cross-section, e.g. hydraulic geometry parameters (width, depth and cross-section area). Maco-scale features are those fluvial forms having dimensions at the scale of the floodplain, e.g. meander geometry and riffle-pool length.
- The rate of change in these features. The rate of change in fluvial systems is measured as a function of (a) change in dimensions of selected meso-scale features relative to a “baseline” value that is averaged over decades for a predefined length of channel (reach); and, (b) change in the “baseline” value under current and future conditions.
- The energy in the fluvial system evaluated relative to (a) resistance of the boundary materials; and, (b) sediment transport potential and the sediment supply.

Change through time in the “baseline” or average dimensions of selected meso-scale features occurs in fluvial systems as they respond dynamically to variations in processes (climate, sediment supply, change in slope, among others). For example consider a channel that progressively downcuts and narrows through resistant and massively bedded bedrock. In such a case, the rate of change in the average value of the channel form is relatively low over decades and the system may be described as having “statistical stationarity” over the these time frames.

Stationarity is most readily apparent in channels with relatively small changes in form provided the change in dimensions oscillates about the average value over time. Stationarity can also be maintained despite large changes in channel form from year to year (for example, alternating wet years to dry years). Large changes in channel form from year to year produce relatively large departures from the average

value and therefore a high variance of the values observed for the feature of interest. Braided channels are examples of channels that undergo significant alterations in form at any point along the channel from year to year but whose average dimensions taken over many years tends to be consistent. Consequently, annual measures of channel form will show significant variability about the average value. Santiago Creek fits this description.

Conversely, channel systems that are relatively constant from year to year produce low variances. For example, some channel types (characteristic of glaciated temperate terrains and the piedmont region in the eastern United States) do not experience significant morphological adjustment during rare flood events. These are typically meander-pool-riffle, cascade-pool and step-pool channel forms. Channel forms that produce large variances are typical in anastomosing and braided channel morphologies. All of these channel types are considered to be in "metastable equilibrium", although the braided and anastomosing channels are more dynamic, as they have a higher degree of variance about the mean.

Metastable equilibrium channels were further classified into watercourses demonstrating "catastrophic[1]" or "regime" behavior. These behaviors differ in that the geomorphically "dominant discharge"[2] for the former channel systems has a higher "recurrence interval"[3] than in regime-type system. Consequently the concept of Effective Work" (Wolman and Miller, 1960) and the "dominant discharge" can be applied to both behaviors.

Systems in metastable equilibrium attempt to maintain a balance between the driving processes controlling channel form and the morphology of the channel. This balance represents an equilibrium state that is disrupted when there is a disturbance in the driving process. The response of the channel to this disturbance depends on the sensitivity of the channel system and the magnitude and duration of the disturbance. Simplified explanations of possible response scenarios are provided below:

A) If the magnitude and duration of the disturbance in the driving process do not exceed the geomorphic threshold for change[4], the system remains in a stable state. Under conditions where the channel materials are highly susceptible to entrainment and transport, the geomorphic threshold will be low. Conversely, the threshold in more robust systems will be higher. In terms of alteration in the sediment-flow regime associated with land use change a greater degree of urbanization may occur before destabilization of the channel occurs in the more robust system;

B) If the magnitude and duration of the disturbance exceed the geomorphic threshold, one of the following responses will occur:
   - The channel returns to its original equilibrium position after cessation of the disturbance; (time scale?)
   - The channel adjusts its morphology to attain a new equilibrium form in keeping with the altered state of the driving process. The new morphology of the channel will be significantly different from the pre-disturbance form of the channel; or,
   - The channel is unable to find a new equilibrium form and continues to adjust, sometimes rapidly and catastrophically. Serrano Creek is an example of such a metamorphsis.

[1] A stream classified as having catastrophic behavior is characterized by geomorphic alteration during rare flood flow events, generally the 1:10 or 1:25 year event.
[2] The flow event that performs the most work in terms of the mass of sediment transported.
[3] Recurrence interval is the number of years on average between occurrences of an event of specified magnitude. For example, a 1:25 year event occurs, on average, every 25 years and has a 4% chance of occurring in any given year,
[4] The concepts described as "metastable" and "threshold" are analogous to endothermic chemical reactions, where a compound that is metastable is reluctant to form a new, stable phase unless a critical activation energy is attained (a sufficiently high disturbance).

The latter response scenario is characteristic of "dis-equilibrium" channel systems. An example of a dis-equilibrium system is a channel having a relatively steep gradient (i.e. a longitudinal gradient greater than or equal to 2 %) within a weakly-indurated sandstone bed and lacking a supply of coarse material (cobble- to boulder-sizes) and Large Woody Debris (LWD) necessary to stabilize the channel. The sandstone is susceptible to weathering through abrasion and spalling from expansion and contraction processes. Given the lack of coarse-grained sediment, the channel cannot form an armor layer that would act as a negative feedback mechanism to control downcutting. Furthermore, LWD that increase channel roughness and traps and retains coarse particles is also absent in many southern California channel systems. Such channels retain their ability to downcut and without an effective negative feedback mechanism, downcutting will continue, forming steep gullies or canyons. Downcutting will continue over decades to centuries if the channel does not intersect a more resistant stratigraphic unit or the gradient (slope) decreases to a point where there is a significant reduction in erosion potential to stabilize the bed.

In terms of stream energy, Brookes (1995) found that channels of different form (Table C1-1) can be related to specific stream power criteria when plotted on a graph regressing channel longitudinal gradient as a function of discharge per unit width of channel (Fig. C1-1). The forms listed below (in Section C1-3) have been proposed by Gregory and Walling (1972), Leopold, et al.(1964), Schumm (1977) and Brookes (1995) among others. Aquafor Beech Limited has adjusted the values adopted for the specific stream power criteria for site-specific conditions including those presented in southern California. However, the criteria should be interpreted as indicative of a single region rather than multiple regions.

All of the stream types and channel forms described in the above discussion exist within the study area. Five different channel types are included in the eleven cases examined, as summarized in Table C1-2.

The specific stream power criteria are applied as summarized in Table C1-3 for the Study Sites. Channel Type based on specific stream power is also compared to field classification of Channel Type to test the reliability of the stream power method. The two methods were found to be in close agreement. It was concluded that the specific stream power method may be used to classify Channel Types in southern California.

C1.3 IMPLICATION FOR STORMWATER MANAGEMENT CRITERIA

Stormwater management options and design criteria are directly related to Stream Type. Dis-equilibrium systems are the most sensitive and any increase in erosion potential will aggravate existing instabilities. Non-shear stress dominated systems vary considerably in their sensitivity to any alteration in the sediment-flow regime, depending upon the proximity of the channel to a threshold with anastomosing systems. This holds for any channel system that is close to the threshold to another channel type. In this regard, anastomosing channel systems are quite sensitive because they occupy a narrow region of stability.

C1.3.1 Meandering Channels

Meandering channels cover three basic morphologies. At the lower gradient-energy level the bed materials tend to be fine-grained and the riffles form short undulations in the bed under the water surface at low flow. Pools are very shallow relative to riffles and both are susceptible to mobilization during a flow event. Under moderately high energy conditions the bed materials are coarser and the riffles increase in length while pools become shorted. Under higher sediment loads the riffles may form runs or glides. The riffles are still mobilized under high flow conditions, although they tend to reform immediately downstream of their former positions. The coarse bed materials may be exposed during low flow periods. Near the upper end of the energy

limit for meander-pool-riffle channels the riffles are very long relative to the pools, which become quite short. The bed materials are composed of coarse-grained particles that form riffle-lines that stabilize the smaller substrate carried by the watercourse. The riffle materials are typically exposed during low flow periods. From this description it is apparent that a continuum of forms exist depending on the availability of coarse material in direct proportion to the increase in flow energy. If these materials are available, an increase in flow energy may cause destabilization of the channel as it adjusts its form to a new equilibrium position. If the supply of coarser material is insufficient, the channel may destabilize and remain unstable until the planform and longitudinal gradient have adjusted to the new sediment-flow regime. Consequently, these systems are more robust than anastomosing channels but still relatively sensitive to any alterations in the sediment-flow regime.

With reference to Figure C1-1, it can be seen that there are a number of channels that lie close to the threshold between Cascade-Pool/Braided and Step-Pool/Canyon morphologies. Systems in close proximity to such a threshold can cross the threshold on wet or dry years, thereby increasing the complexity of resulting channel forms. As noted above, such narrow stability thresholds causes channels to be extremely sensitive to alterations in sediment flow regimes.

C1.3.2 Braided Channels and Cascade-Pool Channels

Braided and cascade-pool streams occupy the same area on the specific stream power criteria graph. However, the two morphologies are very distinct. A braided channel is governed by specific conditions of sediment transport competence and capacity relative to sediment transport potential. The particles are within the competence of the watercourse but the supply of sediment exceeds the capacity of the watercourse to move the material. A decrease in sediment supply coupled with an increase in flow energy can destabilize a braided channel system. If there is sufficient coarse-grained material to armor the channel, the braided channel may evolve into a cascade-pool channel form. However, if armoring material is lacking, the channel will destabilize and remain unstable until it erodes down to a more resistant stratigraphic unit or it reduces its slope through planform adjustment. Consequently, the sensitivity of braided channel systems to urbanization depends on maintaining both an adequate supply of sediment to the channel and the physical size of the particles.

Braided channels also tend to have a high width to depth ratio. This means that any increase in flow is spread out over the channel, producing a proportionately small change in stage of flow. Since the forces exerted in the bed are directly proportional to the depth of flow, braided channels exhibit a greater tolerance to alterations in the sediment-flow regime when compared to meander-pool-riffle morphologies. However, water flows tend to focus where the channel finds a weaker bed material and downcutting ensues. The morphology will change to a single thread channel and downcutting accelerates. This appears to be occurring in Borrego Canyon Wash in the downstream reach at Section BOR(d/s)-02.

Cascade-pool channel morphologies are dependent on the supply of coarse-grained particles sufficient to form riffle lines to stabilize the riffle substrate. Materials deposited *in situ* from bank erosion or particles transported downstream during rare flood flow events may exceed the stream competence, producing an armor layer or lag deposits. These channels have a high tolerance to alteration of the sediment-flow regime.

C1.3.3 Step-Pool Channels and Canyon Channels

Step-pool channel and canyon channel morphologies occupy the highest zone on the specific stream power graph. As with braided and cascade-pool systems, the step-pool and canyon

morphologies are also very distinct. Step-pool channels are dependent on the supply of very coarse particles (cobbles, boulders to massive boulder sizes). The larger particles form imbricated structures that represent riffle- or step-like structures between plunge pools. Large boulders trap and stabilize the intermediate sized bed materials, whilst fine-grained material are typically flushed through the channel system, leaving isolated pockets of sand and gravel materials in the lee of large boulders and imbricate structures. Step-pool channel forms can be very robust with a high tolerance for change in the sediment flow regime. Sediments transported from upland areas (including areas affected by urban development) have little impact on the channel because virtually all the material required to stabilize the channel is recruited from the channel bed itself.

Large Woody Debris (LWD) can be an integral part of these systems, contributing in both positive and negative ways. Debris jams tend to trap material and protect the bed and banks, which is important where the competence of the channel is equal to, or exceeds, the resistance of the coarse-grained sediment. However, where the LWD becomes a structural component of the Step-pool morphology, the failure of the LWD due to rot or poor anchorage can send a flood and accompanying debris wave downstream, thereby initiating a cascade of failures (a domino effect). These failures can de-stabilize the channel. The gradient and width of the channel also play a role in determining the effectiveness of LWD. As the channel increases in both gradient and width, there is a corresponding decrease in the role of LWD in determining channel form diminishes. For example, the presence of LWD in Topanga Creek has a minor role in the determination of channel morphology.

Canyon-type channel systems represent another high-energy channel form, one that lacks the negative feed back mechanisms required to arrest the downcutting process. These channels are dis-equilbrium systems as described above.

C1.4 SUMMARY

In general channel sensitivity to an alteration in the sediment-flow regime is influenced by the following factors:

A) **System Energy**: In general, as system energy increases channel sensitivity to alterations of the sediment-flow regime decreases. The notable exception is the canyon type morphology;
B) **Channel Width to Depth Ratio**: The sensitivity of a channel to alteration of the sediment flow regime decreases as width to depth ratio increases;
C) **Connection To Floodplain**: Similar to (B), channel sensitivity decreases with access to a broad flat floodplain;
D) **Boundary Material Composition**: Channel sensitivity decreases with increasing boundary material size;
E) **Sediment Supply**: In general, channel sensitivity decreases when the supply of sediment available from upstream sources is sufficient to meet sediment transport potential;
F) **Large Woody Debris**: LWD assists in stabilizing the channel if it can effectively trap coarse sediments and increase flow resistance without compromising the channel bed through underflow and eroding the opposite bank through deflection of the flow or the creation of chutes;
G) **Proximity to Geomorphic Thresholds**: Channels whose morphology is near a geomorphic threshold have less tolerance for change than other channel systems all other factors being equal; and,
H) **Catchment Drainage Area**: Channel sensitivity has been shown to be inversely proportional to drainage area.

Table C1-1. Stream Type and Specific Stream Power Criteria

Channel Form[(a)]	Meso-scale Feature	Specific Stream Power[(b)] (Watts/m^2)	Sediment	
			Capacity[(c)]	Competence[(d)]
Canyon	na	$\omega \geq 130$	P > A	P > R
Step-Pool	na		P ≥ A	P < R
Braided	na	$37.5 \leq \omega < 130$	P < A	P > R
Cascade-Pool	na		P > A	P < R
Meander-Pool-Riffle	Exposed Riffle or Run	$3.4 \leq \omega < 37.5$	P ≥ A	P = R
	Emergent Riffle			
	Submerged Riffle			
Anastomosing	na	$2 \leq \omega < 3.4$	P < A	P ≥ R
Non Shear-Stress Dominated	na	$\omega < 2$	P < A	P < A

(a) Channel form categories and descriptions modified after Leopold, et. al (1964), Gregory and Walling (1972), Schumm (1977), and Brookes (1995).

(b) Specific stream power is defined as $\omega = \Omega / W$, or stream power (Ω) per unit width of the channel.

(c) Capacity to transport sediment as represented by total mass for specific particle size fractions.

(d) Competence (resistance) of bank and bed materials as a function of stream power.

P Energy potential of stream to mobilize and transport sediment.

A Actual sediment mobilization and transport as a function of energy potential.

R Resistance of bank and bed material to mobilization and transport.

na Not applicable

Table C1-2: Stream Types and Channel Features Recognized in the Study Area

Watercourse	Section ID	Canyon	Step-Pool		Cascade-Pool		Braided	Meander-Pool-Riffle	
			Riffle	Pool	Riffle	Pool		Riffle	Pool
Topanga	TOP-01		•						
	TOP-02		•						
	TOP-03			•					
Hasley Canyon d/s	HAS-01		•						
	HAS-02		•						
	HAS-03		•						
	HAS-04		•						
Plum (u/s)	PLU(u/s)-01				•				
	PLU(u/s)-02						•		
	PLU(u/s)-03						•		
	PLU(u/s)-04						•		
	PLU(u/s)-05				•				
Plum (d/s)	PLU(d/s)-01						•		
	PLU(d/s)-02						•		
	PLU(d/s)-03						•		
	PLU(d/s)-04							•	
	PLU(d/s)-05							•	
Borrego Canyon Wash u/s	BOR(u/s)-01				•				
	BOR(u/s)-02						•		
	BOR(u/s)-03						•		
	BOR(u/s)-04				•				
	BOR(u/s)-05						•		
Borrego Canyon Wash d/s	BOR(d/s)-01				•				
	BOR(d/s)-02				•				
	BOR(d/s)-03						•		
	BOR(d/s)-04						•		
	BOR(d/s)-05				•				

Table C1-2: Stream Types and Channel Features Recognized in the Study Area

Watercourse	Section ID	Canyon	Step-Pool		Cascade-Pool		Braided	Meander-Pool-Riffle	
			Riffle	Pool	Riffle	Pool		Riffle	Pool
Serrano Creek	SER-01	•							
	SER-02	•							
	SER-03	•							
	SER-04	•							
	SER-05		•						
Santiago Creek	SAN-01								
	SAN-02								
	SAN-03					•			
	SAN-04				•				
	SAN-05		•						
Dry Canyon	DRY-01				•				
	DRY-02				•				
	DRY-03				•				
	DRY-04				•				
	DRY-05		•						
Hick's Canyon	HIC-01		•						
	HIC-02				•				
	HIC-03				•				
	HIC-04				•				
	HIC-05								

Table C1-3. Application of Specific Stream Power Criteria For Channel Stability

Watercourse	Section ID	Field Classification of Channel Type	Bed Material Mobility Based On Excess Boundary Shear Stress Based on ϕ_{84}	Specific Stream Power Criteria	
				Stream Type	Stability Class
Borrego Creek d/s	BOR(d/s)-01	Cascade-Pool	Susceptible to Scour	Cascade-Pool	Unstable
	BOR(d/s)-02	Cascade-Pool	Susceptible to Scour	Cascade-Pool	Unstable
	BOR(d/s)-03	Braided	Susceptible to Scour	Braided	
	BOR(d/s)-04	Braided	Susceptible to Scour	Braided	
	BOR(d/s)-05	Cascade-Pool	Resistant	Cascade-Pool	Stable
Borrego Creek u/s	BOR(u/s)-01	Meander	Resistant	Meander-Pool-Riffle	Stable
	BOR(u/s)-02	Braided	Susceptible to Scour	Braided	
	BOR(u/s)-03	Braided	Susceptible to Scour	Braided	
	BOR(u/s)-04	Braided	Resistant	Braided	
	BOR(u/s)-05	Cascade-Pool	Susceptible to Scour	Step-Pool	Unstable
Serrano Creek	SER-01	Canyon	Susceptible to Scour	Canyon	Unstable
	SER-02	Canyon	Susceptible to Scour	Canyon	Unstable
	SER-03	Canyon	Susceptible to Scour	Canyon	Unstable
	SER-04	Canyon	Susceptible to Scour	Canyon	Unstable
	SER-05	Step-Pool	Susceptible to Scour	Step-Pool	Unstable
Hick's Canyon	HIC-01	Step-Pool	Resistant	Step-Pool	Stable
	HIC-02	Cascade-Pool	Susceptible to Scour	Cascade-Pool	Unstable
	HIC-03	Cascade-Pool	Susceptible to Scour	Meander-Pool-Riffle	Unstable
	HIC-04	Cascade-Pool	Susceptible to Scour	Step-Pool	Unstable
	HIC-05	Cascade-Pool	Susceptible to Scour	Cascade-Pool	Unstable
Plum Canyon u/s	PLU(u/s)-01	Cascade-Pool	Susceptible to Scour	Cascade-Pool	Unstable
	PLU(u/s)-02	Braided	Susceptible to Scour	Braided	
	PLU(u/s)-03	Braided	Susceptible to Scour	Braided	
	PLU(u/s)-04	Braided	Susceptible to Scour	Step-Pool	Unstable
	PLU(u/s)-05	Cascade-Pool	Susceptible to Scour	Step-Pool	Unstable
Plum Canyon d/s	PLU(d/s)-01	Braided	Resistant	Cascade-Pool	Stable
	PLU(d/s)-02	Braided	Susceptible to Scour	Braided	
	PLU(d/s)-03	Braided	Susceptible to Scour	Braided	
	PLU(d/s)-04	Meander	Resistant	Meander-Pool-Riffle	Stable
	PLU(d/s)-05	Meander	Susceptible to Scour	Meander-Pool-Riffle	Unstable

Table C1-3. Application of Specific Stream Power Criteria For Channel Stability

Watercourse	Section ID	Field Classification of Channel Type	Bed Material Mobility Based On Excess Boundary Shear Stress Based on ϕ_{84}	Specific Stream Power Criteria	
				Stream Type	Stability Class
Hasley Canyon	HAS-01	Step-Pool	Susceptible to Scour	Cascade-Pool	Unstable
	HAS-02	Step-Pool	Susceptible to Scour	Step-Pool	Unstable
	HAS-03	Step-Pool	Susceptible to Scour	Step-Pool	Unstable
	HAS-04	Cascade-Pool	Susceptible to Scour	Cascade-Pool	Unstable
Topanga Canyon	TOP-01	Step-Pool	Susceptible to Scour	Step-Pool	Unstable
	TOP-02	Step-Pool	Resistant	Step-Pool	Stable
	TOP-03	Step-Pool	Resistant	Step-Pool	Stable
Dry Creek	DRY-01	Cascade-Pool	Resistant	Cascade-Pool	Stable
	DRY-02	Cascade-Pool	Resistant	Cascade-Pool	Stable
	DRY-03	Cascade-Pool	Susceptible to Scour	Cascade-Pool	Unstable
	DRY-04	Cascade-Pool	Susceptible to Scour	Cascade-Pool	Unstable
	DRY-05	Cascade-Pool	Resistant	Cascade-Pool	Stable
Santiago Creek	SAN-01	Step-Pool	Susceptible to Scour	Cascade-Pool	Unstable
	SAN-02	Step-Pool	Susceptible to Scour	Cascade-Pool	Unstable
	SAN-03	Cascade-Pool	Resistant	Cascade-Pool	Stable
	SAN-04	Cascade-Pool	Susceptible to Scour	Step-Pool	Unstable
	SAN-05	Step-Pool	Susceptible to Scour	Cascade-Pool	Unstable

1. After Brookes (1995)

Figure C1-1 Stream Power vs. Gradient

Stream Power (Discharge/Unit Width) versus Gradient (Longitudinal Slope) for streams within the Study Area. Channels below S3 ($\omega < 37.5$ Watts/m^2) are classified as stable channels of meander pool-riffle morphology. Channels between S3 and S4 (37.5 < $\omega < 130$ Watts/m^2) are braided or cascade-pool channels. Channel with stream power in excess of S4 ($\omega > 130$ Watts/m^2) have step-pool or canyon-forming morphologies.

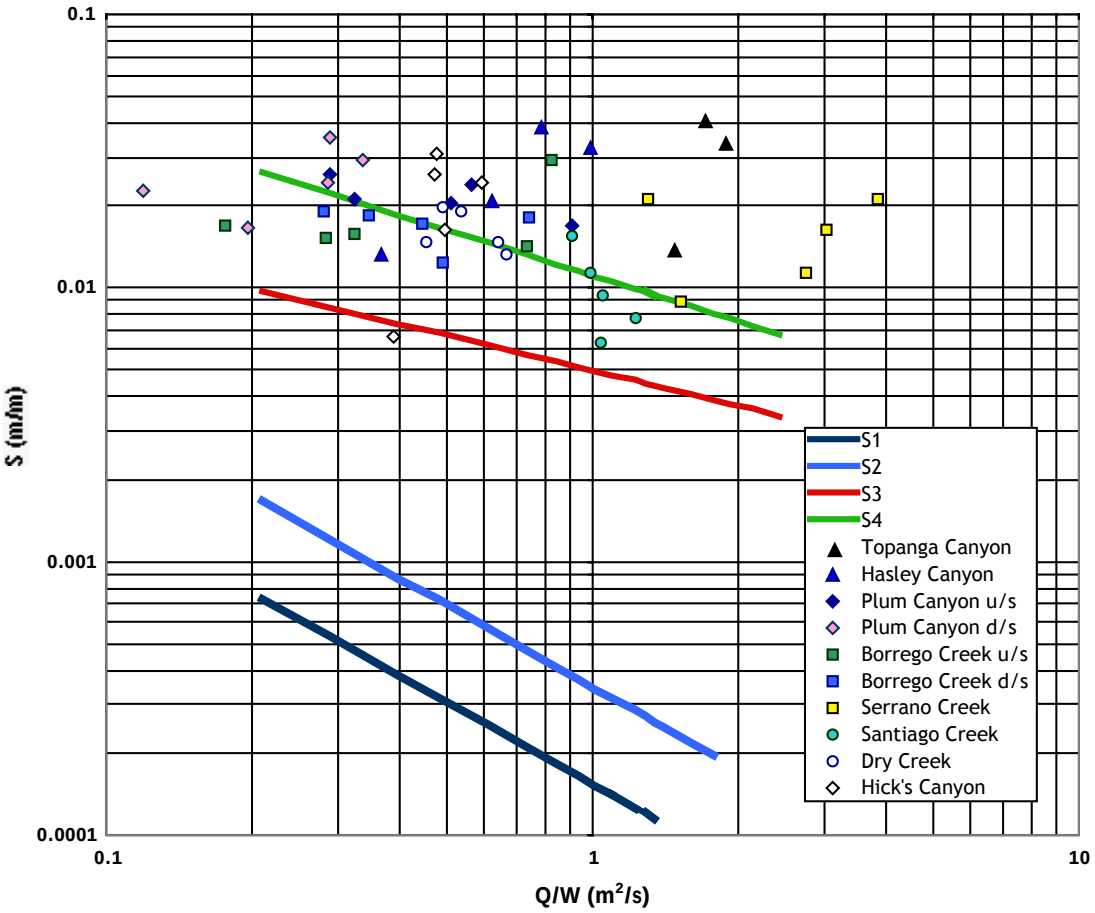

C2. Dominant Discharge Use and Frequency

C2.1 INTRODUCTION

Understanding what constitutes a stable or unstable channel form, how geomorphic thresholds are related to channel stability, and which mode of adjustment a channel will adopt when de-stabilized are fundamental requirements for the management of hydromodification. Such understanding is also key to developing practical and meaningful watershed management programs of which Stormwater Management is a significant component. This Appendix deals with the concepts of stability, stationarity and the dominant discharge, as they relate to natural stream channels.

A stable channel may be defined as one where there is a net balance between the ability to perform work (i.e. capacity to erode), the resistance of the boundary materials of the channel, and the sediment supply it transports. The net result of this balance is that the channel maintains its form through time in a generally similar form. A net balance infers that measures of channel form over periods of decades (engineering time frames) deviate about a mean value but the mean value demonstrates statistical stationarity. This definition is also consistent with the concept of metastable equilibrium form (see Appendix C1) and the definition offered by Watson and others (1999). In their definition a stable stream is characterized as one that has (or is) adjusting its width, depth and slope such that there is no significant aggradation or degradation of the streambed or significant planform changes (e.g. meandering to braided) within an engineering time frame (less than 50 years). By this definition, a stable river is not in a static condition, but rather is in a state of dynamic equilibrium where it is free to adjust laterally through bank erosion and bar building.

Although the channel is formed by a continuum of flows, Wolman and Miller (1960) observed that some measures of channel form could be correlated with a single discharge rate defined by the maximum point on a curve of the product of the frequency of an event and its sediment transport potential. They described this event as the channel forming flow or the "Dominant Discharge." Therefore, the Dominant Discharge is considered to be the single, dominant flow that would produce a channel with the same morphology as that created by a range of flows in a stable channel system exhibiting metastable equilibrium form. As alluded to above this is an over-simplification, in that the channel encompasses a broad spectrum of flows (Leopold, 1968). Nevertheless, this concept can be used to relate morphological trends to a single discharge (Leopold et al., 1964). The critical factor is the determination of what constitutes the dominant discharge in streams that are stable (see discussion by Copeland and others, 2000) or at least metastable within engineering time frames.

In stable channel systems the dominant discharge may be identified from biological indicators and fluvial features. Although there can be considerable scatter in measuring the stage of the dominant discharge at any specific cross-section, this problem can be resolved by taking numerous estimates along the length of the channel and fitting a backwater model such as HEC II to the data. The resulting water surface profile provides a close approximation of the depth of the dominant discharge.

Measurement of the stage of dominant discharge is more problematic in unstable channel systems, where the dimensions of the fluvial features may still be evolving and thus do not necessarily reflect the dominant discharge nor satisfy the condition of statistical stationarity. Stream instability generally occurs as a consequence of an increase of energy or changes in sediment load and/or slope. This results in increased erosion of the streambed and banks, a situation common to urban watercourses that are inherently unstable due to alteration of the sediment-flow regime associated with land use changes. Urban watercourses are also subject to impact through direct alteration of the watercourse (e.g. in-stream channelization, diversion, water-taking and contribution from storm outlets and irrigation return water). Consequently, it may be misleading to define the dominant discharge uniquely on the dimensions or configuration of fluvial forms in urban watercourses where the rate of geomorphic activity is high.

Indeed it was demonstrated in Appendix C1 that most of the streams are unstable, with the possible exception of step-pool morphologies such as Topanga, a situation that calls into question the concept of applying dominant discharge to these streams.

In metastable equilibrium systems the adjustment process tends to be non-uniform with the rate of adjustment initially high, and then declines in a logarithmic manner through time as the channel approaches a new metastable equilibrium position. Consequently, indicators of the dominant discharge may begin to occur relatively early in the adjustment process. However it may be difficult to differentiate between indicators associated with past and present sediment-flow regimes, particularly for low or initial levels of impact. Despite these difficulties, the analyses in Appendix C3 present hydraulic geometry relations and regressions between the dominant discharge and CDA that demonstrate the use of the dominant discharge concept has merit.

The last point of concern for the use of the dominant discharge approach is whether these systems are statistically stationary. It is demonstrated in Appendix C3 that the condition of statistical stationarity is violated for the majority of the sites included in this investigation. This finding precludes the classification of these systems as metastable equilibrium channels, however the geomorphic activity rates associated with this non-stationarity are sufficiently low that the concept is valid when assessed over the engineering time frame of decades.

To validate the applicability of the dominant discharge concept in the study sites, we have explored a surrogate measure, namely the value of the recurrence intervals (RI) for the dominant discharge, calculated from two independent methods:

A) Bio-geomorphic Indicators of the Dominant Discharge (Q_{bfl}) prorated by area to gaged watersheds where the flood frequency curve can be defined from the flow record; and,

B) Application of USGS flood frequency curve relations developed from gaged watersheds.

It appears that a degree of corroboration exists between these two methods, and the derived RI from both approaches falls within the RI for arid climates, which is generally between 2 and 10 years according to Baker and Ritter(1975). Therefore, it is concluded that the concept of dominant discharge is a valid approximation. These methods are discussed in the following sections.

C2.2 DOMINANT DISCHARGE: BIO-GEOMORPHIC INDICATORS

Geomorphic and biotic indicators of the depth of flow at possible Dominant Discharge stages were noted in the field at each cross-section as part of the Diagnostic Survey. Typically, this field procedure entailed five cross-sections with estimates of the dominant discharge on both banks, for ten estimates per survey Reach. Geomorphic indicators include (but are not limited to) terraces, tops of bars, break-of-slope points, changes in composition of overbank deposits and stain lines. Biotic indicators include (but are not limited to) root lines, changes in vegetation type based on tolerance to water, demarcations between vegetated and non-vegetated areas, litter and debris lines, the age of selected tree species, exposed roots and leaning trees.

The estimated depth of the dominant discharge was used to determine the flow rate from stage-discharge relationships developed for the channels at each cross-section. Graphical presentations of the stage-discharge relationships for the Master Cross-sections at each of the eleven Study Sites are provided below (Figures C2-1 to C2-10). A summary of the dominant discharge estimates based on bio-geomorphic indicators is provided in Table C2-1.

C2.3 DOMINANT DISCHARGE: RECURRENCE INTERVAL APPROACH

An estimate of the dominant discharge can be made from a flood frequency curve if the RI value for the dominant discharge is known. A procedure for determining RI values was developed using flow data from gaged watersheds within the study area, and it is described below.

The RI value for the dominant discharge for the gaged basins [$Q_{bfl\text{-}GB}$] was determined by:

1. Constructing flood frequency graphs for each of the gaged basins (as illustrated in Figure C2-11 for Aliso Creek at El Toro);
2. Fitting equations to the flood frequency curves assuming a dual runoff regime concept applies (see Major and Minor flow event relations plotted in Figure C2-11);
3. Finding the value of R_{CDA} defined as the ratio of the Catchment Drainage Area of the gaged watershed to the Study Site ($R_{CDA} = CDA_{bfl\text{-}GB}/CDA_{bfl\text{-}Site}$);
4. Estimating the dominant discharge ($Q_{bfl\text{-}GB}$) for the gaged basin through proration by area defined as the product $R_{CDA} * (Q_{bfl\text{-}Site})$;
5. Finding the corresponding RI value for the gaged basins using the flood frequency curves as illustrated for Aliso Creek at El Toro in Figure C2-11.

A number of gaged watersheds located in the study area were considered for use in determining the recurrence interval for the flows in the Study watercourses. Summary statistics for the gaged watersheds selected for use are provided in Appendix A (Table A3-1). The lengths of record of these gages varies from 25 to 63 years. The above procedure was repeated for each of the Study Sites with the resulting RI values presented in Table C2-2.

The Topanga and Santiago survey sections are located near gaging stations for each watershed. Assuming the estimates of RI from these two Sites are representative of the true recurrence interval value than the RI estimate from Little Tujunga is overestimated by 2.1 and 2.6 times respectively. This may explain the generally higher estimates obtained for RI using the Little Tujunga data (see Table C2-2). Performing the same assessment for Arroyo Simi noted that RI values were 3.4 and 1.4 times higher then the assumed "true" RI values for Topanga and Santiago respectively. However, Little Tujunga estimates were not high for all Survey Sites and this phenomenon may be related to similarities in the hydrophysiographic properties of the gaged and Survey Site watersheds. Consequently a third criterion in the selection of the gaged watersheds is based on the compatibility of hydro-physiographic characteristics. In this exercise the geographical proximity of the gaged basin to the Study Site is used as a surrogate for a more detailed assessment of basin characteristics. The selection of gages based of this criterion is summarized by Study Site in Table C2-2 as represented by the RI values in bold type. The average RI values using "All Stations" and those derived using the "Geographical Proximity Approach" are summarized in Table C2-3 for comparison.

From Table C2-3 it can be seen that Little Tujunga and Arroyo Simi watersheds tend to produce RI estimates that are significantly higher than those derived for other gaged watersheds (see Table C2-3 column 2: "Average RI Value (years)", "All Stations"). Based on this observation and assuming Topanga and Santiago Stations provided a close approximation of the "true" RI value (as noted previously) it was surmised that inclusion of the Little Tujanga and Arroyo Simi watersheds produced an inflated RI estimate. This affect is most pronounced for the "Geographical Proximity Approach" where the Little Tujunga and Arroyo Simi gauging stations were the sole basis for derivation of the RI estimate (see Table C2-3 column 3). The "Revised RI Estimates" computed with exclusion of the Little Tujunga and Arroyo Simi stations are provided in Table C2-3 in column 6 under "All Stations" and column 7 entitled "Geographical Proximity Approach". Comparison of the RI estimates under "All Stations" and the "Geographical Proximity Approach" demonstrates a relatively good agreement between the data sets. The RI estimates in the "All Stations" column tend to be lower than those values reported in the "Geomorphic Proximity Approach" column. However, with the exception of the Topanga and Santiago estimates it could not be concluded that RI estimates based on the "Geomorphic Proximity Approach", excluding Little Tujunga and Arroyo Simi stations, provided the closest approximation of the "true" RI values. Despite the difference in RI values a two sample F-test for variance and the single tail z-test for means

concluded that the two data sets were drawn from the same sample population at the 95% confidence level.

To provide some additional insight into the magnitude of the RI value for the Study Sites an alternative approach was explored. Specifically, relations for the prediction of flood magnitude and frequency for selected recurrence intervals have been developed by the USGS for the south coastal area of the State of California. These relations are as follows:

$$Q_{2YR} = 0.14*CDA^{0.72}P^{1.62} \quad [C2.1]$$

$$Q_{5YR} = 0.40*CDA^{0.77}P^{1.69} \quad [C2.2]$$

$$Q_{10YR} = 0.63*CDA^{0.79}P^{1.75} \quad [C2.3]$$

$$Q_{25YR} = 1.10*CDA^{0.81}P^{1.81} \quad [C2.4]$$

$$Q_{50YR} = 1.50*CDA^{0.82}P^{1.85} \quad [C2.5]$$

$$Q_{100YR} = 1.95*CDA^{0.83}P^{1.87} \quad [C2.6]$$

where the subscript 2YR through 100YR refers to the return period or recurrence interval (RI) of the event, "Q" represents the flow rate (cfs), CDA is the Catchment Drainage Area and "P" is the mean annual precipitation (inches).Using Equations [C2-1] through [C2-6] a flood frequency curve was constructed for each watershed of interest (see for example Fig. C2-12).

Knowing the dominant discharge it is possible to generate an estimate of RI as presented in Table C2-4. These estimates of RI represent a parallel but independent method for comparison with the gaged watershed approach described above.

Unfortunately a simple comparison of the RI estimates between the gaged watersheds and the USGS flood frequency relationships is not possible. The relationship between CDA and RI is complicated by the flow regulation structures and the impact of urbanization on the peak flow rate. As peak flow rate increases with urbanization the higher flows are associated with higher return periods on the pre-development flood frequency curve (see Table C2-5 for Plum Creek as an example). A more representative portrayal of the return period would require modification of the flood frequency curve to reflect the new flow regime. The affect of urbanization would contribute to a departure between the estimates of RI based on the USGS relations by increasing the USGS based estimates.

Fortunately, six of the eleven Study watersheds represent low levels of impervious cover (TIMP). However, the remaining four watersheds have moderate imperviousness values. Taken collectively the average value for the gaged basins was RI_{ave}=3.7 yrs in comparison to RI_{ave}=5.0 yrs for the USGS based estimates. A comparison of the average RI values obtained for the USGS and the gaged watersheds is provided in Table C2-6. A 2-sample F-test for variance indicate that the difference between the sample populations was not significant at the 95% confidence level. However, the z-test for means indicated that the sample populations were likely different at the same confidence level. Consequently, it may be concluded that the two data sets came from different sample populations. The lower value reported for the gaged watersheds may be related to the affect of impervious cover as well as impoundments and possibly diversions on the gaged watersheds used to develop the USGS relations.

It is also important to note that the two data sets have similar distributions although the mean values are offset. The consistency in the sample distributions supports the contention that the concept of a dominant discharge applies to the Study Sites.

C2.4 SUMMARY AND CONCLUSIONS

As a result of this review, we conclude the following:

1. Calculating recurrence intervals using two different methodologies provides a useful confirmation of the estimated values as well as for the concept of dominant discharge;
2. Recurrence intervals estimated for the established Q_{bfl} values range between 4 and 40 years, which is anticipated from streams in arid climates;
3. The concept of using dominant discharge as a comparitive value is appropriate for unstable streams in Southern California within engineering time frames (measured in decades);
4. There are significantly larger values of Q_{bfl} RI for watersheds with catchment drainage areas between 35 and 70 square miles.

Table C2-1 Estimates of the Dominant Discharge
Based on field identification of bio-geomorphic indicators in May 2004

Watercourse	CDA (mi^2)	TIMP (%)	Dominant Discharge - Q_{bfl} (cfs)					
			Sect-01	Sect-02	Sect-03	Sect-04	Sect-05	Average
Topanga Creek	18.07	2.8	1,423.0	1,381.4	1,477.9			1,427.4
Hasley Canyon	1.66	3.4	68.4	77.5	73.2			73.0
	1.55	1.3				64.8		64.8
Plum Canyon	2.23	17.0	241.1	286.4	237.5	337.4	308.2	275.6
	2.40	17.5	144.3	127.8	123.7	123.0	120.3	129.7
Borrego Canyon Wash	2.27	22.0	329.8	361.2	327.7	351.4	347.3	342.5
	3.06	21.0	260.5	221.7	269.6	237.3	228.8	247.3
Serrano Creek	2.64	26.7	328.4	321.0	347.6	344.4	358.9	335.3
Santiago Creek	12.36	0.2	754.4	701.3	807.0	766.5	731.3	757.3
Dry Canyon	1.22	0.7	52.3	51.7	67.0	62.3	55.5	58.3
Hick's Canyon	1.33	1.2	44.3	37.9	44.0	44.3	44.1	42.9

Table C2-2a. Summary of Recurrence Interval Estimates
Based on the Dominant Discharge from the study watersheds using the proration-by-area method with selected gaged watersheds.

Gage Station Number	Stream	CDA (mi^2)	Recurrence Interval (years)				
			Site 1	Site 3	Site 4u	Site 4d	Site 7 u
11047500	Aliso Creek	7.9	3.4	2.4	5.3	2.7	**7.0**
11075800	Santiago Creek	13.0	4.4	2.9	5.5	3.9	**6.4**
F54C-R	Topanga Creek	16.0	**2.0**	1.5	2.9	1.6	3.6
11104000	Topanga Creek	18.0	**2.4**	1.6	5.1	1.8	6.0
11096500	Little Tujunga Ck.	21.1	6.1	**3.3**	**9.8**	**4.0**	6.0
11105850	Arroyo Simi	70.6	8.1	**3.6**	**21.2**	**4.7**	38.4
	Average (all data)		4.4	2.5	8.3	3.1	13.6
	Average (bold)		2.2	3.5	15.5	4.4	6.8
	Data Points (N)		6	6	6	6	6
	Maximum		8.1	3.6	21.2	4.7	20.4
	Minimum		2.0	1.5	2.9	1.6	3.6

Table C2-2b. Summary of Recurrence Interval Estimates
Based on the Dominant Discharge from the study watersheds using the proration-by-area method with selected gaged watersheds.

Gage Station Number	Stream	CDA (mi^2)	Recurrence Interval (years) Site 7 d	Site 9	Site 10	Site 23	Site 27
11047500	Aliso Creek	7.9	**3.4**	**5.5**	3.0	2.5	**2.2**
11075800	Santiago Creek	13	**4.4**	**5.7**	**4.1**	3.4	**2.3**
F54C-R	Topanga Creek	16	2.0	2.9	1.9	1.6	1.4
11104000	Topanga Creek	18	2.4	4.1	2.0	1.7	1.4
11096500	Little Tujunga Ck.	21.1	12.1	16.7	8.6	**18.9**	8.3
11105850	Arroyo Simi	70.6	8.0	22.9	5.5	**4.1**	3
	Average (all data)		5.4	9.6	4.2	5.4	3.1
	Average (bold)		3.9	5.6	4.1	11.5	2.2
	Data Points (N)		6	6	6	6	6
	Maximum		12.1	22.9	8.6	18.9	8.3
	Minimum		2.0	2.9	1.9	1.6	1.4

Table C2-3. Gage Selection for Estimation of RI Values
Based on geographical proximity

Col. 1	Average RI Value (years)		Value of RI (years) For:		Revised RI Estimates[1] (years)	
Study Site	Col. 2 **All Stations** [2]	Col. 3 **Geographical Proximity Approach** [2]	Col. 4 **Little Tujunga**	Col. 5 **Arroyo Simi**	Col. 6 **All Stations**	Col. 7 **Geographical Proximity Approach**
Borrego u/s	13.63	6.68	20.40	38.44	5.74	6.68
Borrego d/s	5.39	3.9	12.12	7.89	3.05	3.9
Plum u.s	8.3	15.51	9.77	21.24	5.71	-
Plum d/s	3.13	4.38	4.03	4.73	2.5	-
Topanga	4.4	2.38	6.11	8.11	3.05	2.38
Hasley	2.54	3.45	3.28	3.63	2.08	-
Serano	9.62	5.57	16.65	22.88	4.54	5.57
Santiago	4.20	4.08	8.63	5.53	2.25	4.08
Dry	5.35	11.51	18.88	4.14	2.27	-
Hick's	3.08	2.23	8.26	2.96	1.81	2.23

(1) Little Tujunga and Arroyo Simi Removed.
(2) Shaded cells indicate Little Tujunga and Arroyo Simi were used in the determination of RI estimates

Table C2-4. Recurrence Interval Estimates for Dominant Discharge
Using the USGS flood frequency relations for the southern coastal region of California

Study Site	Section	Date of Survey	Dominant Discharge Q_{bfl} (cfs)	Estimate of RI	
				USGS Regional Equations (yrs)	Proration By Area (yrs)
Topanga Creek	TOP-02	1-Nov-00	1,731.0	30.7	
		4-May-04	1,381.4	38.0	4.1
Hasley Canyon	HAS(u/s)-04	2002	61.7	5.9	
upstream		22-Feb-03	71.6	6.8	
		14-Mar-03	76.8	7.2	
		29-Mar-03	72.0	6.8	
		19-Apr-03	72.4	6.8	
		9-May-04	64.8	7.2	2.5
Hasley Canyon	HAS(d/s)-02	1990	50.9	5.1	
downstream		6-Oct-01	48.0	5.8	
		1-Dec-01	50.1	6.1	
		14-Dec-02	52.7	6.4	
		28-Dec-02	50.3	6.1	
		9-May-04	77.5	7.2	2.5
Plum Canyon	PLU(u/s)-05	2-Oct-01	50.9	3.2	
upstream		1-Jan-02	48.0	5.8	
		3-Sep-02	50.1	6.1	
		14-Nov-02	52.7	6.4	
		23-Dec-02	50.3	6.1	
		10-Mar-03	59.7	7.2	
		20-Mar-03	47.0	5.7	
		11-May-04	308.2	7.9	5.7
Plum Canyon	PLU(d/s)-02	1990	49.3	3.6	
downstream		2-Oct-91	49.3	3.6	
		19-Jan-03	49.7	3.7	
		22-Feb-03	52.9	3.9	
		14-Mar-03	62.0	4.5	
		29-Mar-03	125.6	8.9	
		10-May-04	127.8	10.2	

Table C2-4. Recurrence Interval Estimates for Dominant Discharge
Using the USGS flood frequency relations for the southern coastal region of California

Study Site	Section	Date of Survey	Dominant Discharge Q_{bfl} (cfs)	Estimate of RI	
				USGS Regional Equations (yrs)	Proration By Area (yrs)
Borrego Canyon Wash upstream	BOR(u/s)-03	1983	106.0	6.6	
		1990	107.3	6.7	
		1-Sep-92	111.8	7.0	
		1-Apr-93	164.2	10.2	
		1-Jan-98	164.5	10.3	
		2001	224.9	14.5	
		1-Jan-03	221.6	14.2	
		6-May-04	327.7	14.4	5.4
Borrego Canyon Wash downstream	BOR(d/s)-03	1972	103.0	4.5	
		1983	103.1	4.6	
		1990	106.1	4.7	
		1-Sep-92	106.1	4.7	
		1-Apr-93	120.4	5.2	
		2001	214.0	9.1	
		7-May-04	269.6	11.6	4.0
Serrano Creek	SER-03	1-Jan-97	153.5	7.4	
		7-May-04	347.6	18.5	
Serrano Creek	SER-04	1-Sep-91	125.0	6.1	
		1-May-03	153.4	7.4	
		7-May-04	344.4	17.8	
Serrano Creek	SER-05	1978	106.5	5.2	
		1982	116.2	5.7	
		1990	127.8	6.1	
		1993	106.1	5.2	
		1-Oct-97	152.8	7.3	
		2001	340.1	17.3	
		7-May-04	358.9	18.5	6.5
Santiago Creek	SAN-01	28-Apr-95	775.0	15.3	
		13-May-04	754.4	14.8	
Santiago Creek	SAN-02	28-Apr-95	926.8	18.9	
		13-May-04	701.3	18.5	
Santiago Creek	SAN-04	28-Apr-95	766.4	15.1	
		13-May-04	766.5	15.1	3.3

Table C2-4. Recurrence Interval Estimates for Dominant Discharge

Using the USGS flood frequency relations for the southern coastal region of California

Study Site	Section	Date of Survey	Dominant Discharge Q_{bfl} (cfs)	Estimate of RI	
				USGS Regional Equations (yrs)	Proration By Area (yrs)
Dry Canyon	All stations	1998	48.4	5.9	
		2-Oct-01	50.9	6.1	
		1-Jan-02	48.0	5.8	
		3-Sep-02	50.1	6.1	
		14-Nov-02	52.7	6.4	
		23-Dec-02	56.3	6.8	
		10-Mar-03	59.7	7.2	
		20-Mar-03	47.0	5.7	
		11-May-04	51.7 – 67.0	7.9	2.7
Hick's Canyon	HIC-04	1-Sep-86	53.4	6.0	
		1-Apr-92	53.2	6.0	
		1-Apr-93	53.4	6.0	
		2001	54.0	6.1	
		2002	54.0	6.1	
		2003	54.0	6.1	
		8-May-04	44.3	6.2	
Hick's Canyon	HIC-02	1-Sep-86	54.6	6.0	
		1-Apr-92	53.4	6.0	
		1-Apr-93	53.4	6.0	
		2001	53.4	6.1	
		8-May-04	37.9	6.1	

Table C2-5. Increase In Recurrence Interval With Urbanization
For Plum Canyon using USGS flood frequency relations derived for the southern Coastal Region of the State of California

Date	TIMP (%)	Q_{bfl} (cfs)	Recurrence Interval (yrs)
12-Jun-05	0.20	49.32	3.6
2-Oct-91	0.20	49.32	3.6
19-Jan-03	0.27	49.71	3.7
22-Feb-03	1.64	52.91	3.9
14-Mar-03	3.79	61.98	4.5
29-Mar-03	15.05	125.64	8.9
10-May-04	17.52	144.31	10.2
10-May-04	17.52	145.31	10.3
10-May-04	17.52	146.31	10.4
10-May-04	17.52	147.31	10.5
10-May-04	17.52	148.31	10.5

Table C2-6. Summary of RI Values for Dominant Discharge Estimates
Using USGS flood frequency relations for the coastal region of southern California and selected gaged watersheds in the Study Area

Study Watershed	USGS Relations RI (yrs)	Gaged Watersheds RI (yrs)
Topanga Creek	n/a	2.4
Hasley Canyon d/s	6.2	2.1
Hasley Canyon u/s	6.6	2.1
Plum Canyon u/s	3.9	5.7
Plum Canyon d/s	7.3	2.5
Borrego Canyon Wash u/s	10.5	6.7
Borrego Canyon Wash d/s	6.6	3.9
Serrano Creek	2.8	5.6
Santiago Creek	1.5	4.1
Dry Canyon	6.4	2.3
Hicks Canyon	6.0	2.2
Average	5.8	3.7
Maximum	10.5	6.7
Minimum	1.5	2.1
Variance	6.3	2.9

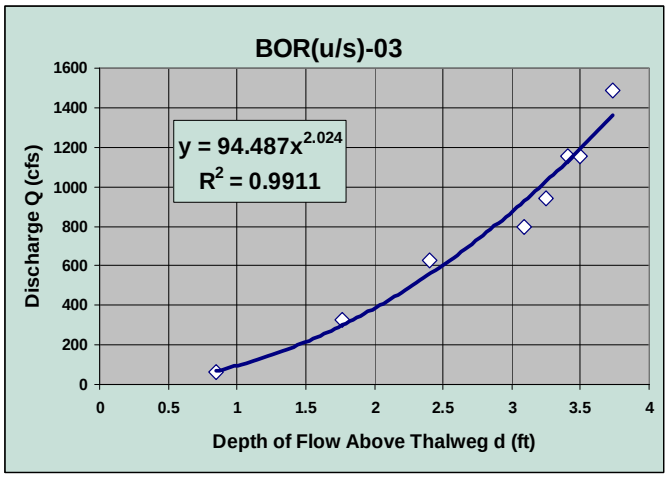

Fig. C2-1. Stage-Discharge Curve: BOR(u/s)-03

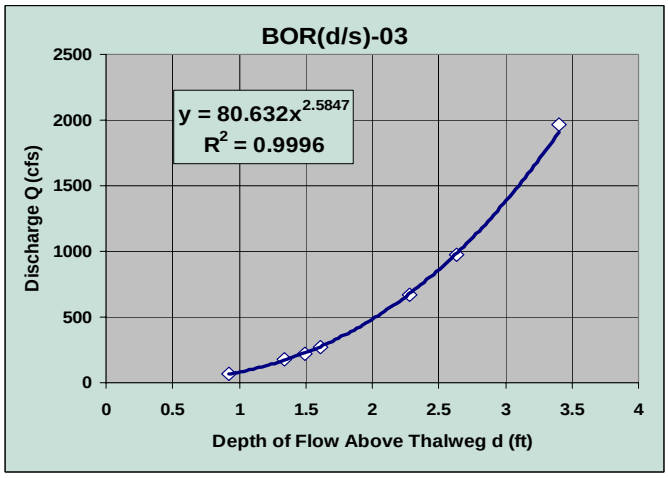

Fig. C2-2. Stage-Discharge Curve: BOR(d/s)-03

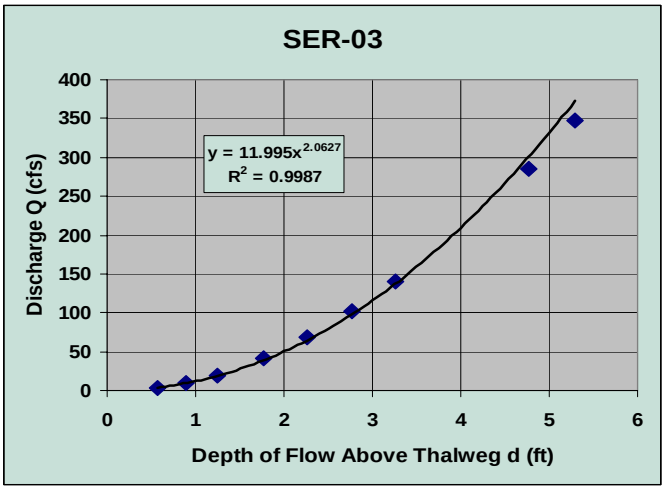

Fig. C2-3. Stage-Discharge Curve: SER-03

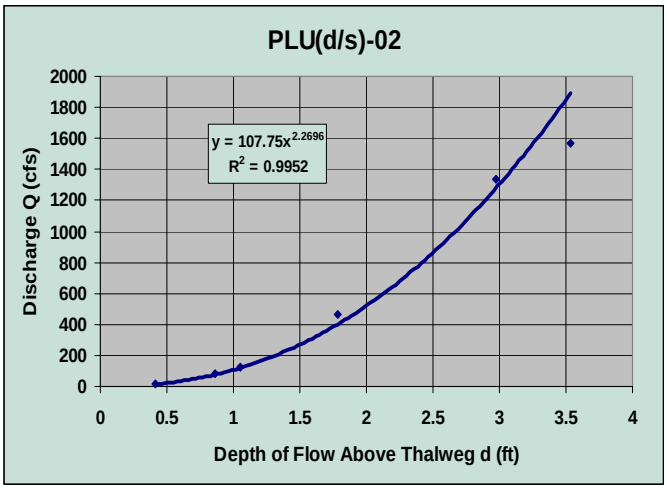

Fig. C2-4. Stage-Discharge Curve: PLU(d/s)-02

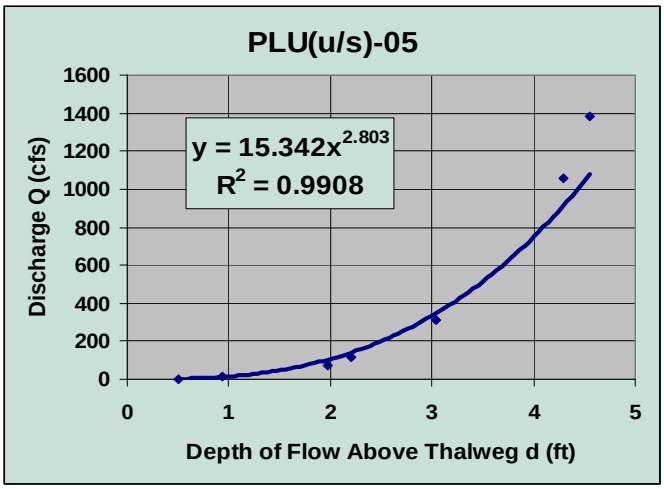

Fig. C2-5. Stage-Discharge Curve: PLU(u/s)-05

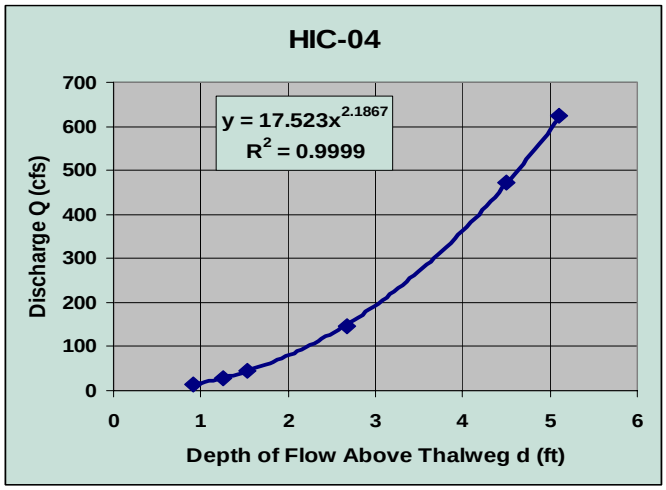

Fig. C2-6. Stage-Discharge Curve: HIC-04

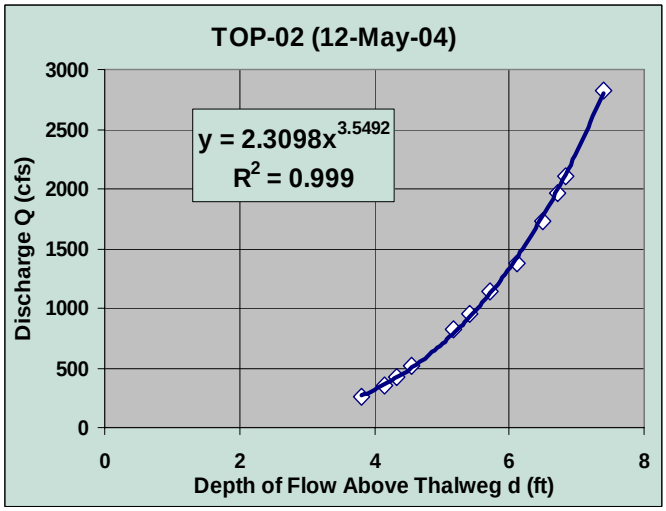

Fig. C2-7. Stage-Discharge Curve: TOP-02

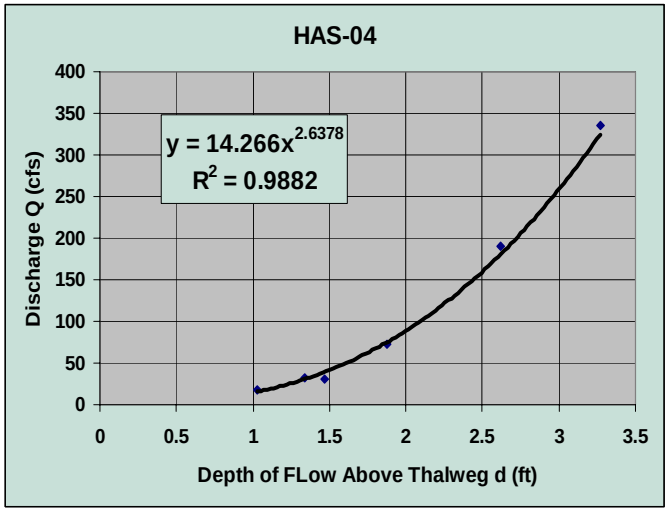

Fig. C2-8. Stage-Discharge Curve: HAS-04

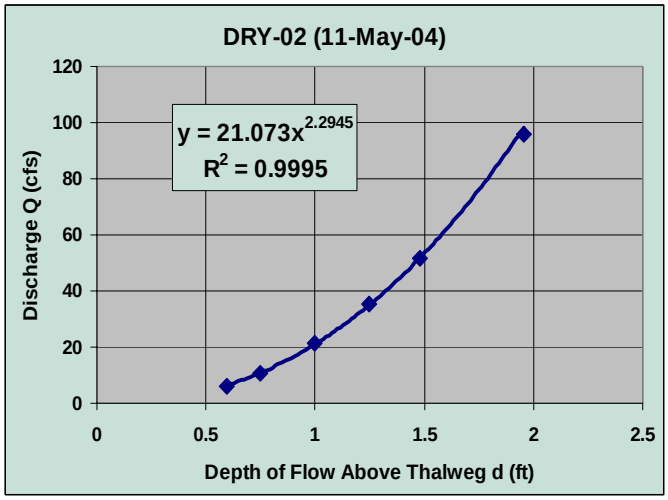

Fig. C2-9. Stage-Discharge Curve: DRY-02

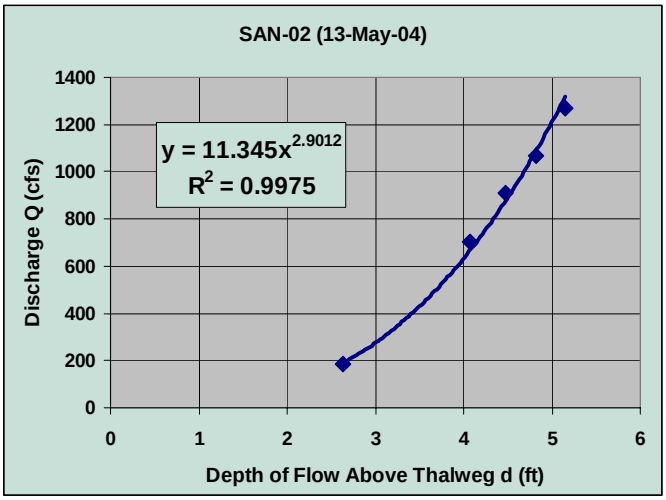

Fig C2-10. Stage-Discharge Curve: SAN-02

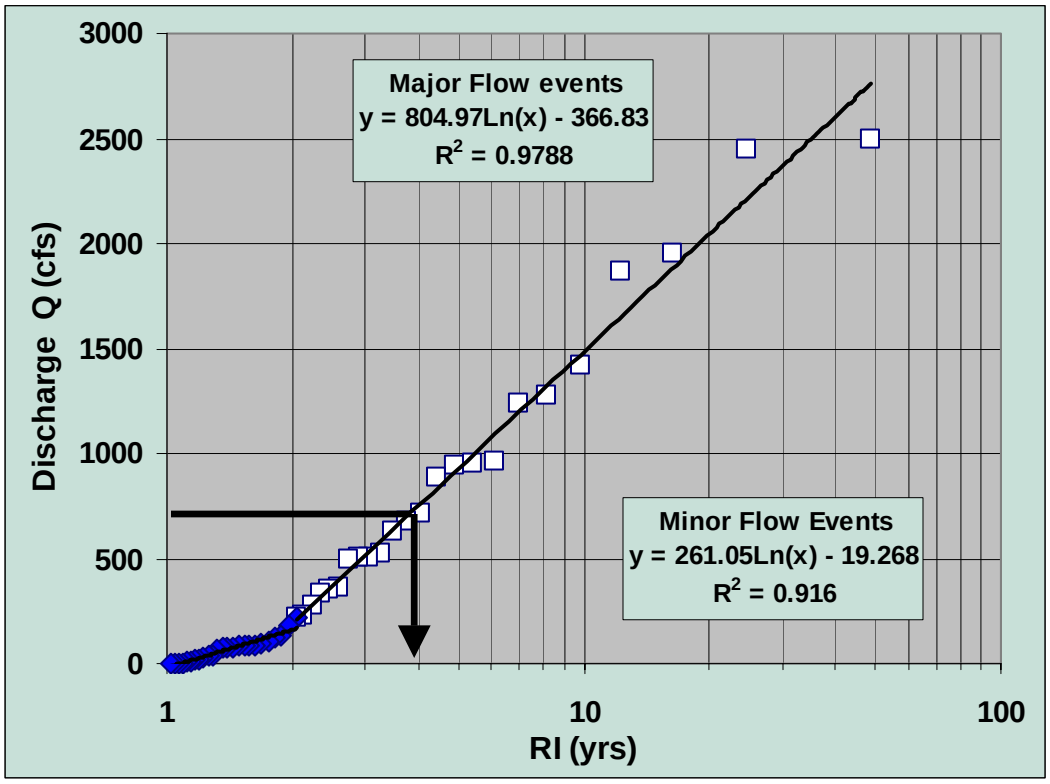

Fig. C2-11. Flood Frequency Curve for Aliso Creek at El Toro, California, Illustrating the Dual Runoff Regime Concept.

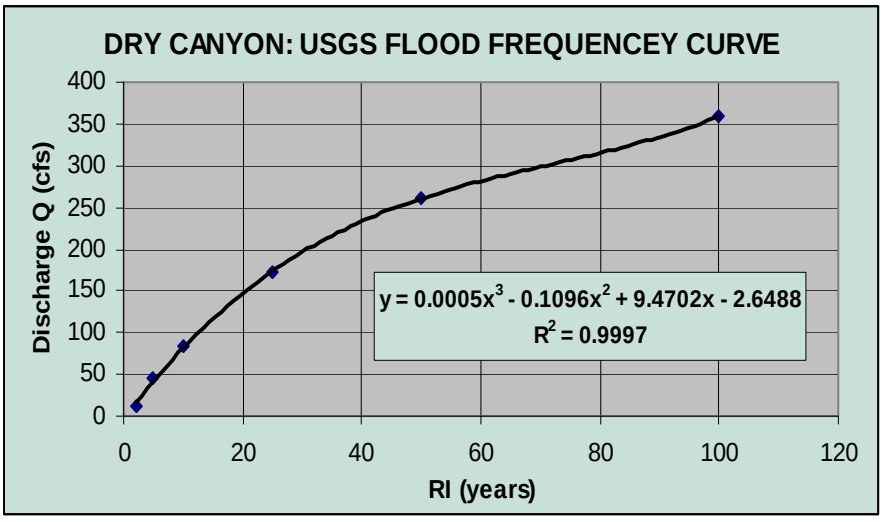

Fig. C2-12. Flood Frequency Curve For Dry Creek Using USGS Relations For the South Coastal Region of California

C3. Form and Process in Southern California Stream Channels

C3.1 INTRODUCTION

In developing the arguments for SWM criteria it is necessary to demonstrate that the channels in Southern California behave in a predictable or deterministic manner. One way to demonstrate this behavior is to show that well-defined relationships between form and process exist for the southern California watercourses under investigation. Since deterministic behavior does not apply to all watercourses it is necessary to identify which channels can be expected to behave in such a deterministic manner and those that are not. A classification system has been proposed for this purpose is described in Appendix C1. Channels that are classified as stable Regime Type or metastable equilibrium systemdemonstrate deterministic behavior. Such systems demonstrate statistical correlations between dominant discharge and hydraulic geometry parameters such as width, depth, cross-sectional area and mean velocity. These relations are of the form,

$$W_{bfl} = a(Q_{bfl})^b \quad [C3.1]$$

$$d_{bfl} = c(Q_{bfl})^f \quad [C3.2]$$

$$A_{bfl} = i(Q_{bfl})^j \quad [C3.3]$$

$$v_{bfl} = k(Q_{bfl})^l \quad [C3.4]$$

Where W_{bfl} = Width of the channel at the dominant discharge stage (feet)

d_{bfl} = Average depth of flow at the dominant discharge stage (feet)

A_{bfl} = Cross-section area at the dominant discharge stage (square feet)

v_{bfl} = Velocity of flow at the dominant discharge stage (feet)

Q_{bfl} = Dominant discharge at the dominant discharge stage (cfs)

a, c, i, k = Coefficients derived for each data set

b, f, j, l = Exponents derived for each data set

Secondly, systems in metastable equilibrium that are classified as stable exhibit statistical stationarity in the average values for the above measures of channel morphology over engineering time scales (decades). A temporal trend in the average value implies progressive alteration in channel form that violates the condition of statistical stationarity.

Finally, systems in metastable equilibrium display relationships between the susceptibility to scour of bank material and the ratio of width to depth. It must be emphasized that the database under consideration is composed predominantly of urban watercourses that are known to be unstable – this will add a degree of scatter to the relationships between form and process. However, the level of development and time frame for adjustment to the disruption in the sediment-flow regime are such that the changes in morphology should be relatively small. Consequently, the above relationships should still apply.

These relationships are presented in the following Sub-Sections of this appendix.

C3.2 HYDRAULIC GEOMETRY RELATIONSHIPS

C3.2.1 Bankfull Width

The relationship between channel width (at the stage of dominant discharge) and the dominant discharge is illustrated in Figure C3-1 for all channel Types and all survey Sites considered in this investigation. As anticipated considerable scatter was noted in the plot and a poor fit was obtained with the power function ($R^2 = 0.5415$). The reason for the poor fit is inclusion of all stream Types in the plot. Stream Type is based on differences in channel morphologies. In this case the majority of channels are AL-Type including gravel bed rivers of meander-pool-riffle, cascade-pool and braided channel forms of single and multiple thread channel structures. Other channel forms include AL(Ar)-Type (Step-pool with armored beds composed of lag deposits – Topanga Creek) and Canyon-Type systems with channels worn into bedrock materials (Serrano Creek).

A re-plot of the data by Study Site (Figure C3-2) shows that the scatter is primarily associated with some sections in Plum Canyon and Borrego Canyon Wash, which plot above the fitted line and Serrano Creek and Topanga Creeks, which plot below the line. Although the Borrego and Plum Canyon channels are AL-Type the outliers were of multiple channel morphology with very high width:depth ratios. Serrano Creek in contrast, is a Canyon-Type channel worn into sandstone bedrock. The Serrano cross-sections exhibit a very low width:depth ratio. The Topanga Creek Site is of Step-pool morphology, which tends to produce a lower Width:depth ratio because of the greater flow depths and shorter widths than the AL-Type channels.

The Topanga channels (AL(Ar)-Type) were included with AL-Type channels in Figure C3-3 because of the smaller difference in morphology and the benefit of extending the abscissa. However, the multiple channel and Canyon-Type channels were sufficiently distinct with respect to channel width that their exclusion from the data set was considered warranted. An explanation for this position is provided in the following Sub-Section. A plot of all single thread AL-Type channels (including the AL(Ar) systems) is provided in Figure C3-3.

Removal of the multiple channel and Canyon-Type data points from the data set significantly increased the fit of the power function ($R^2 = 0.855$). It was noted that a logarithmic representation of the data provided a better model of the relationship between width and the dominant discharge ($R^2 = 0.928$). This may be an artifact of the limited size of the data set or due to inclusion of the AL(Ar)-Type channels.

C3.2.2 Bankfull Depth

Similar plots of depth (at the stage of the dominant discharge) versus dominant discharge are illustrated in Figures C3-4 (all data for all stream Types), C3-5 (all data by Study Site) and C3-6 (Removal of Serrano Creek data).

The curve fitted to the data in Figure C3-4 produced a square of the coefficient of correlation of $R^2 = 0.465$ indicating a poor fit. A re-plot of the data by Study Site noted that Serrano Creek data produced outliers located well above the fitted line (FigureC3-5). The plotting position for the Serrano Creek data was anticipated given the low width to depth (W/d) ratio for Canyon-Type channels. A plot of depth as a function of dominant discharge with Serrano Creek data removed is presented in Figure C3-6. The power function fitted to the data produced a square of the coefficient of correlation of $R^2 = 0.548$ indicating a moderately poor fit to the data.

It was noted that a linear model provided a better fit to the data ($R^2 = 0.703$). The better fit obtained with the linear model may be in part do to inclusion of Topanga Creek data. The depths associated with Step-Pool channel morphologies tend to be higher than reported for AL-Type channels. Consequently depths for Step-Pool channels would plot above the fitted line as shown in Figure C3-4.

C3.2.3 Cross-Section Area

Cross-section area (A_{bfl}, estimated for bankfull depth) for all channel Types and all Study Sites is plotted in FigureC3-7 as a function of the Dominant Discharge. The power function fitted to the data produced a square of the coefficient of correlation of $R^2 = 0.925$, indicative of a very good fit.

The strong correlation between cross-section area and discharge supports the use of A_{bfl} as a measure of impact associated with alteration of the flow regime due to urbanization. The application of the relation established in Figure C3-7 across Stream Type means that the Enlargement Approach is universally acceptable as a means for assessment of the impact of urbanization on channel form. Figure C3-8 identifies the data points by site.

C3.2.4 Flow Velocity

A plot of average primary flow velocity (estimated for the depth of the dominant discharge) as a function of the Dominant Discharge is provided in Figure C3-9 for all data and all stream Types. No regression relationship was discernable from these data.

Re-plotting the data by Study Site (Figure C3-10) shows that the plotting positions for the Serrano Creek data are well above the fitted line. This is consistent with higher flow velocities in Canyon-Type channels with relatively smooth boundaries. However, removal of the Serrano Creek data did not result in a statistically significant regression relationship between v_{bfl} and Q_{bfl}. There was no justification for removal of other outliers based on stream Type. Due to the nature of the data set, it was not possible to differentiate between urban and non-urban sites.

C3.3 BOUNDARY MATERIAL RESISTANCE

The W/d ratio of channels at the stage of the dominant discharge is an important diagnostic criterion because the discharge and sediment supply characteristics determine cross-section area while the W/d ratio is the result of many factors and relationships (Leopold, et. al 1964, Gregory and Walling 1972, and Schumm 1977). Consider the following relationships:

a) Sediment supply versus channel capacity to perform work as represented by sediment transport potential;

b) Sediment size versus stream competence as determined by the absolute resistance of the boundary materials (τ_{crt}) in relation to the instantaneous applied stress (τ_0) at the dominant discharge. This condition is represented by excess shear stress concepts (Equation [C3.5]),

$$\tau_e = (\tau_0 - \tau_{crt}) \qquad [C3.5]$$

in which τ_e represents the excess boundary shear stress;

c) The relative resistance of the bed materials to the bank materials as expressed in Equation [C3.6],

$$\tau_R = (\tau_0 - \zeta\tau_{crt})_{bed} / (\tau_0 - \xi\tau_{crt})_{bnk} \qquad [C3.6]$$

Where τ_R = Ratio of excess bed shear stress to excess bank shear stress

ζ = Bed material imbrication factor

ξ = Bank material root binding factor

and the subscripts "bed" and "bnk" refer to the bed and bank station at points "P" and "Q" about the channel respectively; and,

d) The degree of incisement;

An understanding of the W/d ratio in combination with a function for determination of cross-section area and boundary roughness is sufficient to develop a deterministic model for the subject watercourses. This model may be coupled with a conceptual model governing channel adjustment for prediction of the impact of an alteration of the sediment-flow regime on channel form. The following is a general outline of a possible structure for W/d ratio portion of such a predictive tool.

Step 1: Resolve the relationship between sediment supply and sediment transport potential

For example, where the stream has the competence but lacks the sediment transport capacity to move its sediment load an aggrading condition occurs and sedimentation features dominate channel morphology. This is represented by Lane's (1955) inequality,

$$(Q_S)_{\phi_i} > QS \qquad [C3.7]$$

in which the sediment supply or mass (Q_S) for particles of diameter ϕ_i that are at or less than the competence of the stream exceed the transport potential (QS) for that particle size (Q is the discharge and S is the longitudinal channel slope). If these particles form a significant component of the total sediment load than an aggrading condition will dominate.

Aggradation results in the formation of massive bar deposits that may merge to completely cover the bed, fill pools and cover riffle segments. Increase in the bed elevation places additional stress on the banks. This can result in widening of the channel producing a higher W/d ratio. Aggrading conditions may also be a precursor to a multiple channel form (i.e. a braided channel).

Where stream competence and capacity is sufficient to move the sediment load erosion features dominate channel form. Erosion potential as represented by excess shear stress concepts can be used to explain the channel W/d ratio.

Step 2: Resolve the relationship using balance of forces concepts

In order to understand the relationship between the resistance of the boundary materials and the applied stress, the balance of forces were examined. An equation based on excess boundary shear stress concepts was developed for the Study Sites as illustrated in Figure C3-11 and as provided below.

$$W / d_{ave} = m\{[(\tau_0 - \zeta\tau_{crt})_{bed} / (\tau_0 - \xi\tau_{crt})_{bnk}]\omega\}^b \qquad [C3.8]$$

in which ω represents specific stream power and the parameters ξ and ζ are greater than or equal to un Equation [C3.8] includes:

a) Stream energy per unit width of channel as represented by specific stream power;
b) The absolute resistant of the bed and bank materials in relation to instantaneous shear stress as represented by the term $(\tau_0-\zeta\tau_{crt})_{bed}$ and $(\tau_0-\xi\tau_{crt})_{bnk}$; and,
c) The relative resistance of the bed to the bank material as represented by the quotient of the two terms presented in (b) above.

The square of the coefficient of correlation was $R^2 = 0.67$, which is actually quite good in light of the number of significant factors influencing the W/d relationship.
Consistent and predictable relationships between bank material resistance (as measured by the W/d ratio) and channel morphology provide further indication that the channels under investigation behave in a deterministic manner.

Bank material resistance is a key variable in Equation [C3.8]. This variable can also be used in a stand-alone manner to estimate the W/d ratio as a means of verification of estimated values using Equation [C3.8]. Bank material resistance was determined using Torvane measurements and SCORE values, derived from standard soil consistence tests of stickiness, plasticity and firmness (Center for Watershed Protection 2003). The relationship between SCORE and vane shear strength is presented in Figure C3-12. SCORE values can be converted directly into boundary shear stress values using a transformation function developed by the Study Team

Torvane measurements taken at the Master Cross-Sections for the Study Sites was converted into boundary shear stress values using the relationship with SCORE. The resulting values were plotted against W/d to derive the relationship illustrated in Figure C3-13. As anticipated, the W/d ratio increases as the resistance of the bank material decreases. The fitted regression line produces a reasonable correlation ($R^2 = 0.814$).

Another relationship considered to be of merit is a function capable of predicting the substrate composition. Substrate particle size determined in the field using pebble count and sieve methods are used to derive Manning's "n" (roughness coefficient) by solving the Limerinos (1970) equation. A relationship was developed as Equation [C3.9] for the purpose of predicting ϕ_{84}.

$$\log (d/k_1\phi_{84}) = (k_2 Q_{bfl}\, d^{k_3}) / (AR^{k_4}S^{k_5}) - k_6 \qquad [C3.9]$$

Where
- d = Average depth of flow at the stage of the dominant discharge (feet)
- ϕ_{84} = Particle size fraction for which 84% of the sample is finer by mass (inches)
- A = Cross-section area at the stage of the dominant discharge (square feet)
- R = Hydraulic radius, or the length of the "wetted perimeter" (feet)
- S = Longitudinal slope of the energy gradeline
- k_i = Coefficients of calibration.

Application of Equation [C3.9] using the ϕ_{84} data from pebble counts at the Study Sites produced a strong correlation (Figure C3-14, $R^2 = 0.89$) between predicted and observed data. When combined with the hydraulic geometry relationships, the data support the contention that real and deterministic relationships exist between boundary material resistance to erosion, channel form and the dominant discharge.

C3.4 STATISTICAL STATIONARITY

Statistical stationarity is a state where the average properties of a system do not change with time although variations about the average value may occur from year to year. In hydrologic (and geomorphic) processes, there is often a lag time. In such cases, where it can be demonstrated that stationarity exists in both the mean value and in the covariance of the lag time, a second-order stationarity exists (Haan, 1977). Statistical stationarity is also a condition for metastable equilibrium channels. In such channels a line fitted through a plot of the average value for W_{bfl}, d_{bfl}, A_{bfl}, and v_{bfl} through time would have a slope of zero. If the data plotted in such a manner generated a line with slope of greater than, or less than zero, then the data would generate a trend through time of increasing or decreasing values respectively.

We have demonstrated that the majority of channels in the Study Area are unstable, yet behave in a predictable or deterministic manner over time scales of years to decades. This is illustrated in the case of Dry Canyon, a baseline (non-urban) watershed. Cross-section geometry for the Dry Canyon section DRY-02 was recorded on 8 occasions over a period of 2.61 years between 02-Oct-02 and 11-May-04. The resurveyed cross-sections taken during this period are compared in Figure C3-15.

Change in the height of the thalweg is presented in Figure C3-16. The section exhibits an abrupt downcutting beginning in late 2002. The values of the hydraulic geometry parameters observed for each period are summarized in Table C3-1 and presented graphically in Figure C3-17. The downcutting portrayed in Figure C3-16 is concomitant with increases in the dominant discharge, depth of flow and mean velocity and decreases in cross-section area and width. However, cross-section area had returned to the pre-disturbance state by the end of the 2.61 year period. The other parameters such as flow rate and depth of flow have remained elevated but in balance with a decrease in channel width. The period of observation provides insight into the dynamic behavior of these channel systems but the monitoring period is too short to be definitive.

The increase in runoff can be explained by the increase in runoff generation that accompanies the occurrence of brush fires. Major fires burned through Dry Canyon in the late summer and fall of 2003. However, a rationale for the changes observed between Dec-02 and Mar-03 was not apparent in the rainfall record or associated with the brush fires. Total Basin Imperviousness was constant through the period. Although these changes in hydraulic geometry values violate stationarity the response of the channel was consistent with a metastable equilibrium system. Similar abrupt changes at about the same time were observed in Hick's Canyon, Santiago and Plum, pointing to a regional change rather than a watershed-scale phenomenon.

In contrast, the behavior of an urbanized stream (Plum Canyon) is illustrated in Figure C3-18. The values for the hydraulic geometry parameters are summarized in Table C3-2. During a period spanning 2001 through 10-May-04 urbanization within the watershed caused basin imperviousness to increase from less than 2 percent to over 17 percent. The dominant discharge rate increased from approximately 100 cfs to over 300 cfs during this period. Average primary flow velocity (v_{ave}) initially decreased from approximtely 4.4 fps to about 4.2 fps before increasing dramatically to approximately 6.6 fps. The depth of flow increased and then remained relatively constant. The changes in width and channel cross-section area were more complex. Both width and cross-section area initially increased before decreasing dramatically. The decreases in area and width were associated with a decrease in thalweg elevation and entrenchment of the channel. A conceptual model of channel adjustment for gravel bed-rivers is provided in the following Sub-Section. Although generally applicable this conceptual model would require further adjustment and evaluation before it can be applied to southern California channels. It does, however provide an example of a conceptually based process-response model from which form may be determined.

C3.5 DISCUSSION AND CONCLUSIONS

A review of eleven Study Sites in eight watersheds confirms that significant correlations exist between measures of hydraulic geometry and the Dominant Discharge. These are of sufficient strength to indicate that the systems under investigation conform to metastable equilibrium behavior.

The measures of hydraulic geometry exhibit some well-defined trends through time that, on first glance, violate the conditions of stationarity. Part of this behavior may be attributed to the impact of urbanization on channel form. The classical response of a channel to an increase in the flow regime and a decrease the supply of sediment is downcutting in the incipient stages of adjustment. The conceptual model for channel adjustment to a disturbance in the sediment flow regime, as proposed by Andrews (1979), is as follows:

Phase 1: Thalweg Re-Alignment

As flow rate and volume of runoff increase concurrently with a sediment supply decrease, the ability of a channel to perform work increases. Both trends are likely as a watershed is urbanized. Therefore, the initial response of a channel is the following:

i) The thalweg straightens;

ii) The bed topography levels through removal of bar forms, degradation of riffles, destruction of imbricate structures and filling of pools; and

iii) The bed materials homogenize along the length of the channel through redistribution of the riffle substrate and bar materials.

The changes in channel form that result from these responses include a reduction in channel roughness and a steepening of the effective slope of the channel. This provides positive feedback to the system by enhancing the capacity of the channel to perform work.

Phase 2: Enlargement of the Active Channel

Given the increase in flow energy and the positive feedback response in Stage 1, the initial response of Stage 2 is to downcut where the bed materials are most susceptible to scour. By increasing the conveyance capacity of the channel through downcutting, the effective flow depth increases, along with the flow rate, both of which are contained (constrained) within the active channel. This initial response is also a positive feedback mechanism, increasing the ability of the channel to perform work. The same holds true (although to a lesser degree) in stream channels that respond through widening.

This phase of the enlargement process may involve multiple episodes of downcutting and widening and further increase in the active channel and its conveyance capacity. However, there comes a time when the active channel becomes so wide events that were previously erosive in nature become so attenuated that they are now depositional. These flows begin to concentrate within the bottom of the enlarged active channel and resume downcutting.

The first consequence of continued or cyclical channel downcutting is over-steepening of stream banks, which ultimately leads to failure and the introduction of massive sediment loads to the channel. The morphological response of the channel to a sudden influx of sediment is complex, in that it depends on the competence and capacity of the stream systems relative to the supply of sediment and its resistance to transport. Downcutting may be temporarily halted while the load of sediment is being processed in the channel. However, the net result is an increase in channel cross-section area and its capacity to convey flow and hence perform work. The channel will thus clear itself of the sediment in relatively short order and resume downcutting. During episodes of downcutting the channel may in fact narrow in width, increase in flow velocity and decrease in cross-section area. In gravel bed-rivers this response is normally temporary due to oversteepening and collapse of the banks.

Phase 3: Plan Form Adjustment

The process of enlargement of the active channel continues until the channel is sufficiently wide that flows previously able to erode the boundary are so spread out to be incompetent and actually depositional. These flows begin to concentrate in the channel bed scouring out a new or incipient active channel within the expanded original active channel. The later (or original) active channel is now the incipient floodplain of the new active channel.

The smaller flows begin to create a meandering channel in the incipient floodplain by reworking the loose sediments in the bottom of the channel into bars that act as deflectors during higher flow events. The defectors help widen the channel by increasing bank erosion, which introduces more sediment into the channel while also increasing the magnitude of flows that are now incompetent. This process continues

until the frequency of occurrence of an event capable of reworking the bar deposits is sufficiently large that the bars become vegetated and stabilized. At this point the enlargement process is essentially complete and the incipient floodplain has enlarged to contain a rare flood flow event, e.g. the 1:100 year event. The incipient active channel has stabilized its hydraulic geometry and is now the adjusted active channel.

The above model applies to steeper reaches under adjustment. The model would be different for less steep channel segments because they receive the massive influx of sediment from the upstream segments. This phenomenon has occurred in Borrego Canyon Wash following the 1992 flood and in Plum Canyon (d/s) with enlargement of Plum Canyon (u/s).

Table C3-1. Changes in Hydraulic Properties of Dry Canyon (Section DRY-02)

Date	TIMP (%)	Depth d_{bfl} (ft)	Dominant Discharge Q_{bfl} (cfs)	Width W_{bfl} (ft)	Area A_{bfl} (ft^2)	Thalweg Elevation (ft)	Velocity v_{bfl} (ft/sec)
02-Oct-01	0.7	0.99	40.9	14.5	11.7	86.51	3.41
01-Jan-02	0.7	1.00	48.0	16.9	12.7	86.47	3.16
03-Sept-02	0.7	1.00	50.1	18.9	11.8	86.47	6.12
14-Nov-02	0.7	1.03	52.7	16.8	13.1	86.48	3.27
23-Dec-02	0.7	1.14	56.3	15.0	11.4	86.31	3.46
10-Mar-03	0.7	1.51	59.7	9.19	10.4	85.25	4.62
20-Mar-03	0.7	1.89	47.0	10.7	9.4	84.92	5.28
11-May-04	0.7	1.48	65.8	9.8	11.4	84.75	4.96

Average Rate of downcutting = 0.7 feet/year

Maximum rate of downcutting = 5.0 feet/year

Table C3-2 Changes in Hydraulic Properties of Plum Canyon (Section PLU u/s-05)

Date	TIMP (%)	Depth d_{bfl} (ft)	Dominant Discharge Q_{bfl} (cfs)	Width W_{bfl} (ft)	Area A_{bfl} (ft^2)	Thalweg Elevation (ft)	Velocity v_{bfl} (ft/sec)
1993	0.15	-	-	-	32.7	-	-
2000	0.05	-	-	-	32.7	-	-
2001	0.16	-	101.3	-	32.7	-	-
2003	1.73	-	105.6	-	-	-	-
17-Jan-04	17.0	2.90	302.5	98.7	72.7	100.95	4.12
07-Feb-04	17.0	2.97	301.4	101.2	71.4	100.80	4.23
10-May-04	17.0	6.04	308.2	31.7	46.7	100.32	6.60

Average rate of downcutting = 1.6 feet/year

Maximum rate of downcutting = 1.9 feet/year

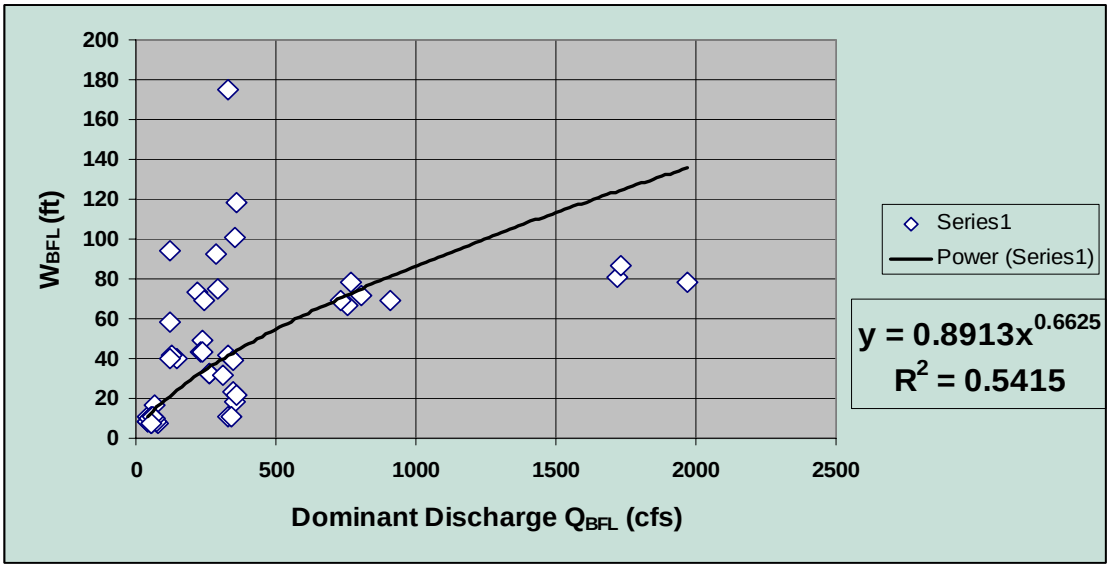

Fig. C3-1. Bankfull Width versus Dominant Discharge for all Study Sites

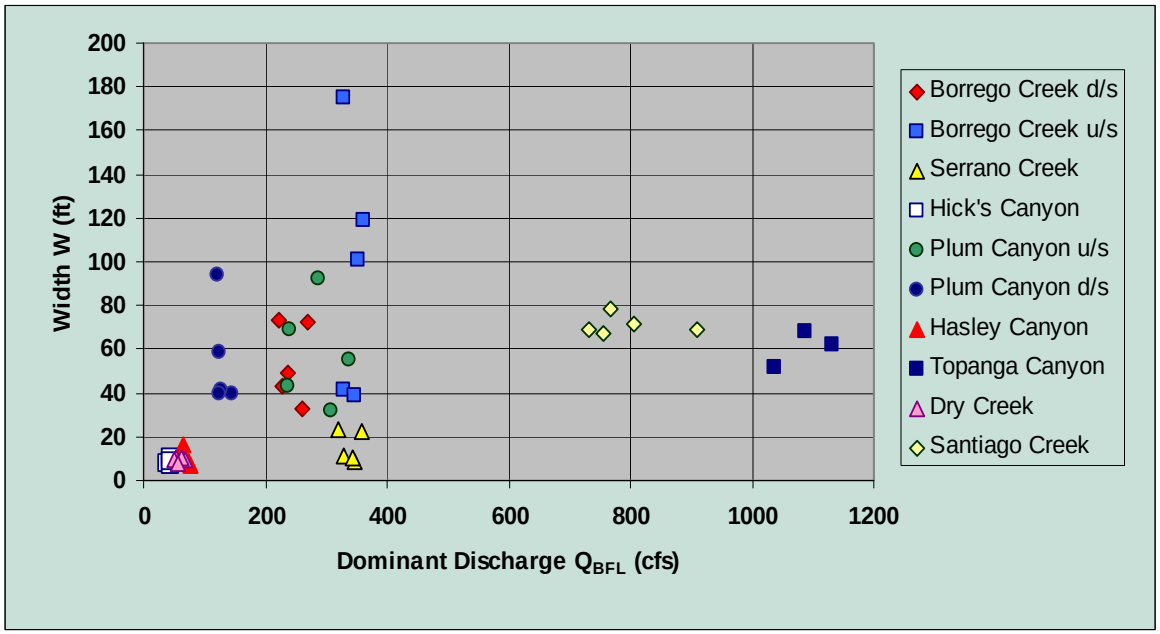

Fig. C3-2. Bankfull Width versus Dominant Discharge by Study Site

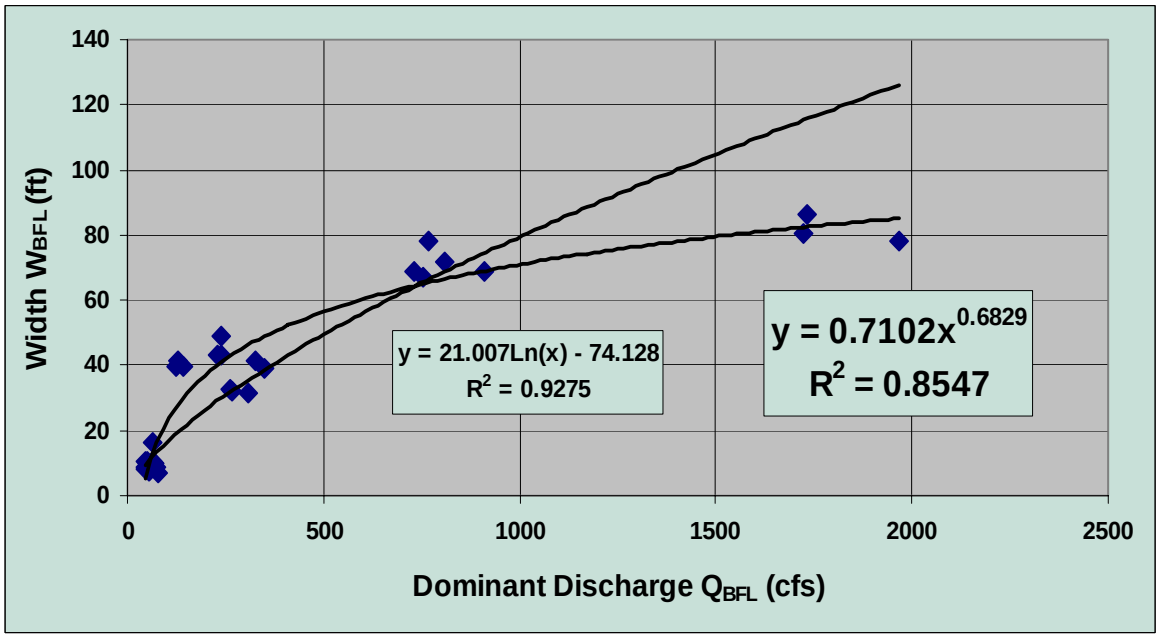

Fig. C3-3. Bankfull width versus Dominant Discharge for all Study Sites (except Borrego Canyon and Plum Creek)

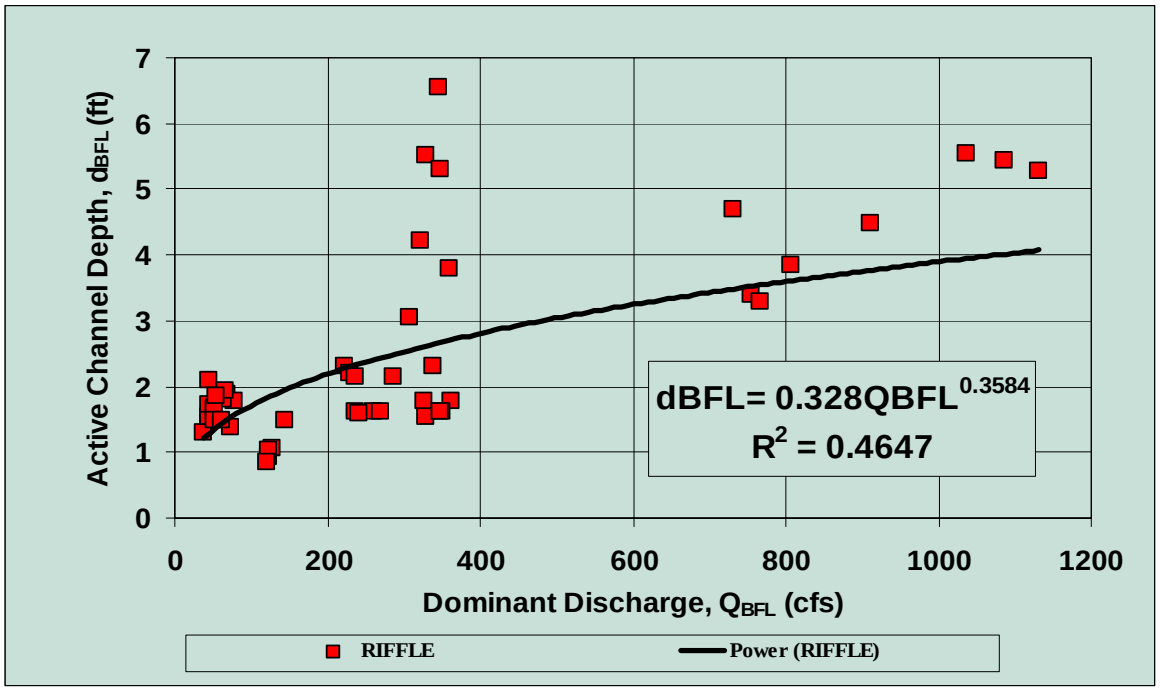

Fig. C3-4. Depth versus Dominant Discharge for Data from All Study Sites

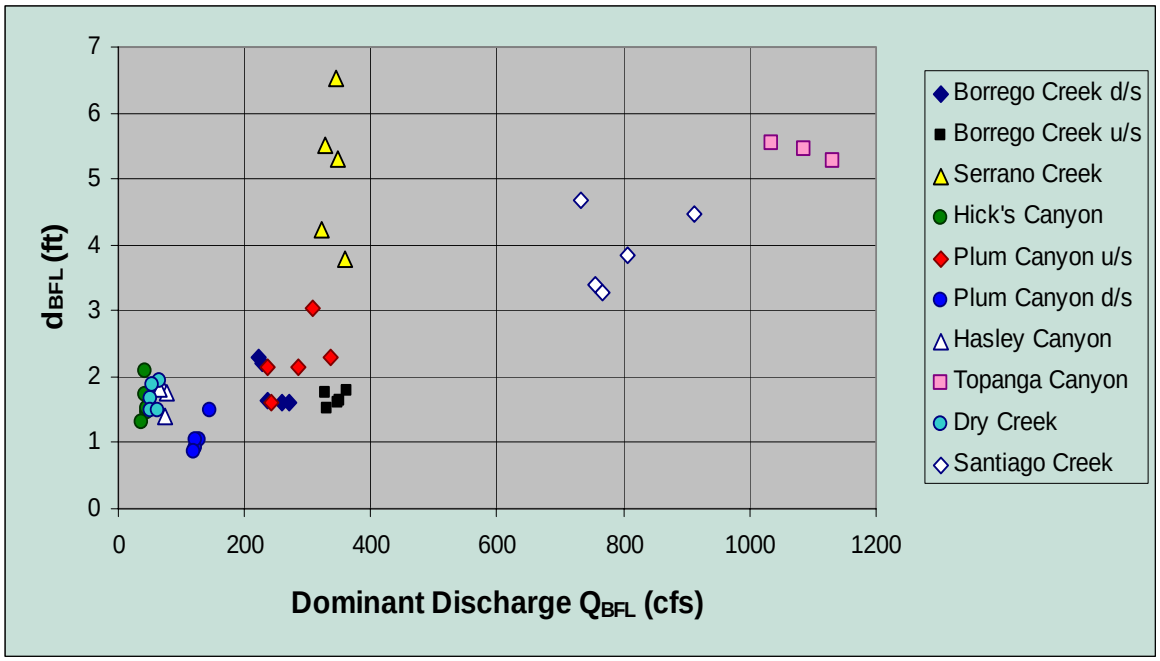

Fig. C3-5. Plot of Depth (at the Stage of the Dominant Discharge) As a Function of the Dominant Discharge (Determined from Field Estimates Based on Bio-Geomorphic Indicators) Organized by Study Site.

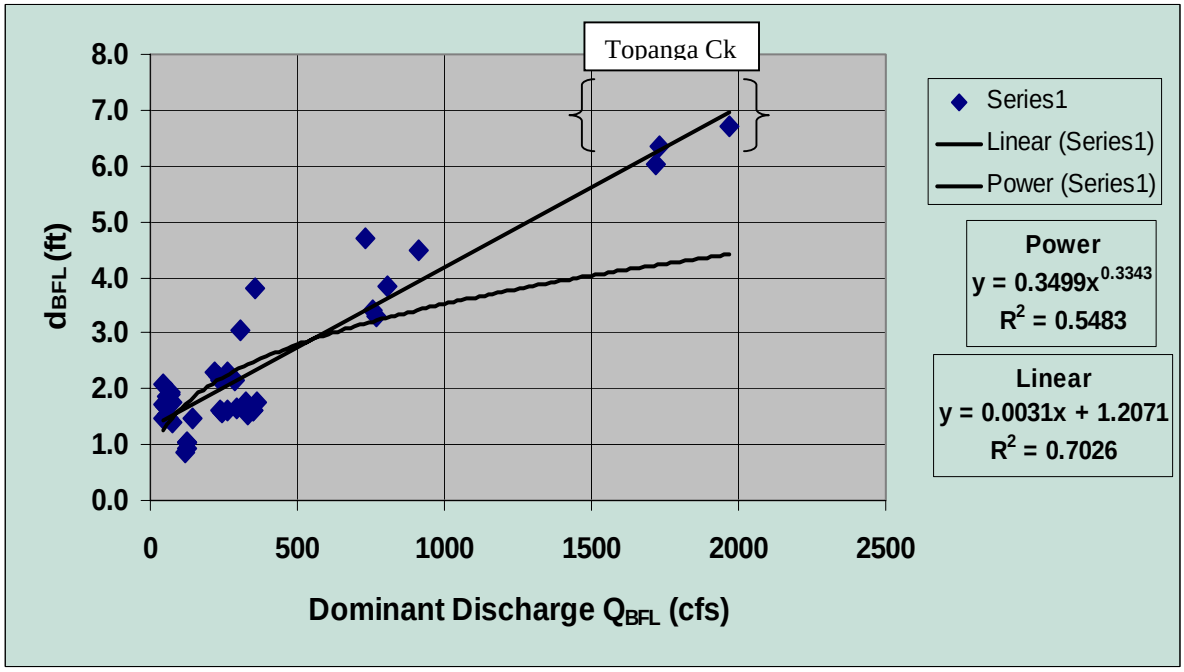

Fig. C3-6. Relationship Between d_{BFL} and Q_{BFL} for AL-Type Channels (Serrano Ck a Canyon-Type Channel has been Removed).

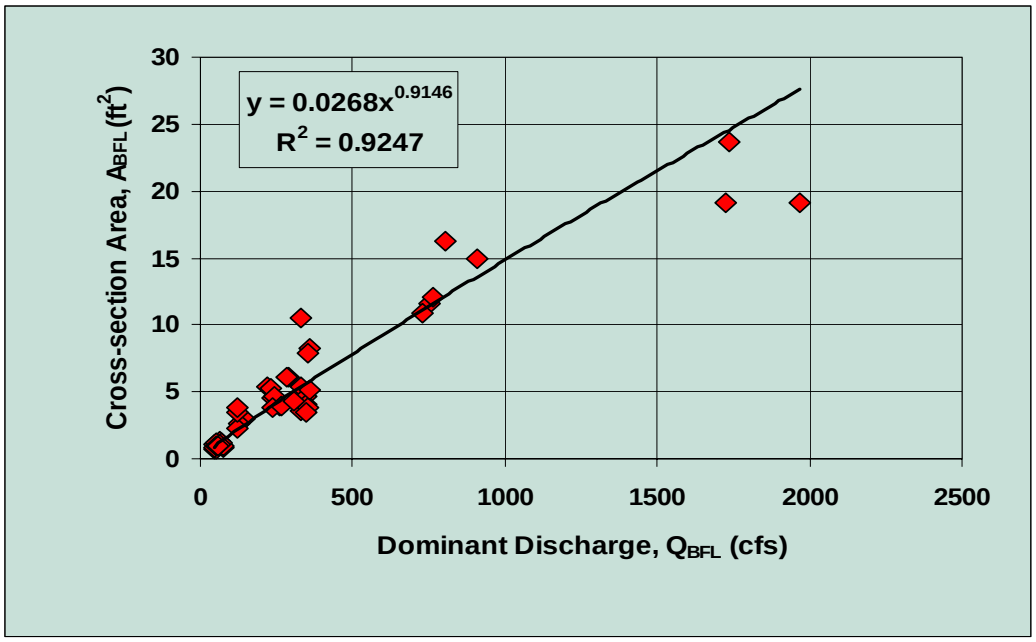

Fig. C3-7. Cross –Section Area versus Dominant Discharge for all Study Sites

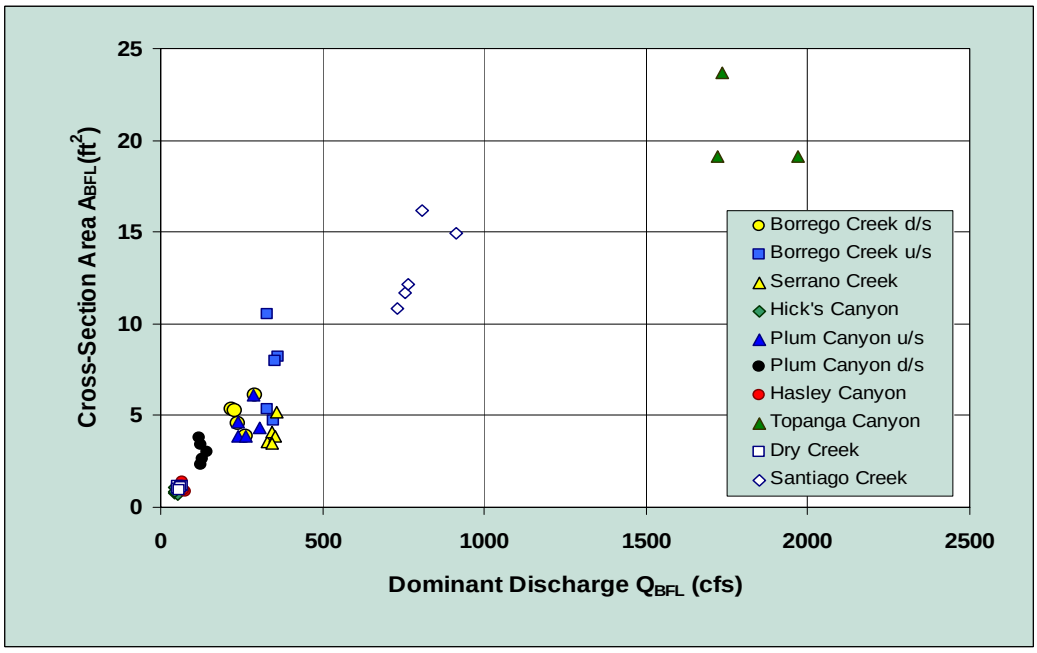

Fig. C3-8. Cross-section Area (At the Depth of the Dominant Discharge) As a Function of the Dominant Discharge for All Data Organized by Study Site.

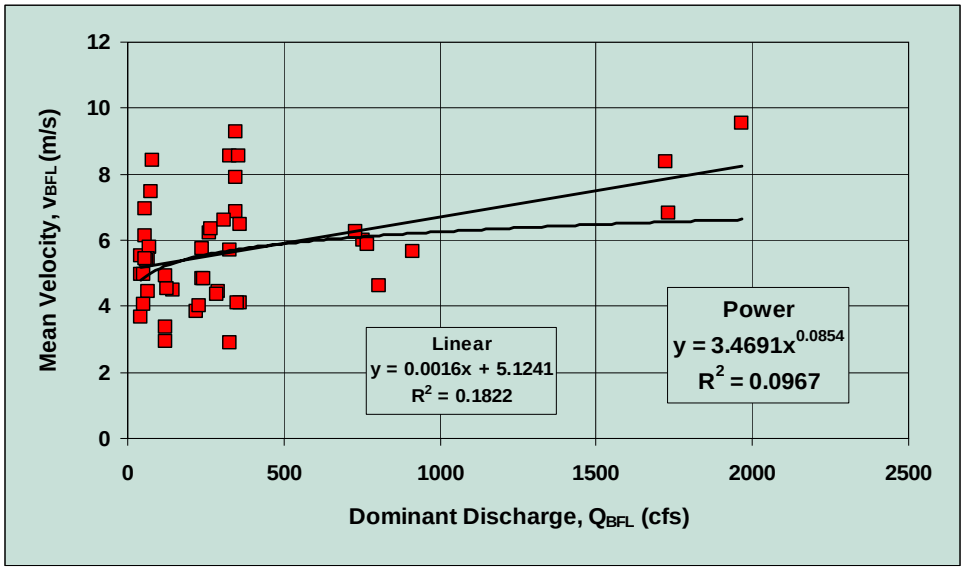

Fig. C3-9. Mean Flow Velocity versus Dominant Discharge for all Study Sites

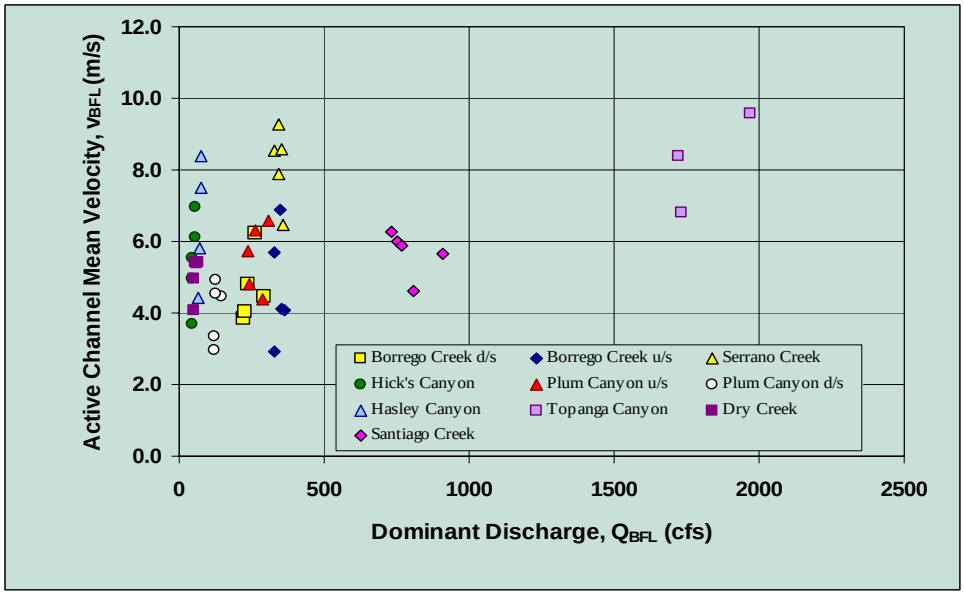

Fig. C3-10. Average Primary Flow Velocity vs Dominant Discharge by Study Site

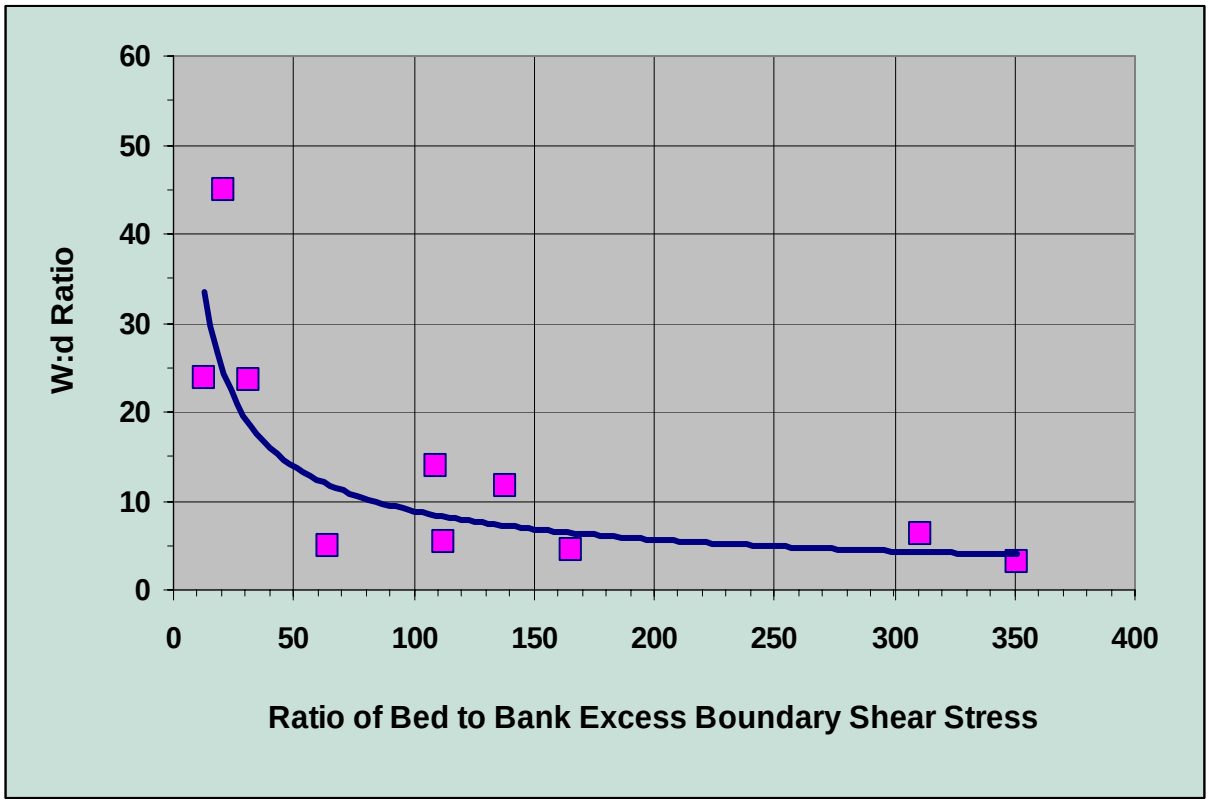

Fig. C3-11. Width: Depth Ratio As a function of the Product of Specific Stream Power and the Ratio of Bed to Bank Excess Boundary Shear Stress

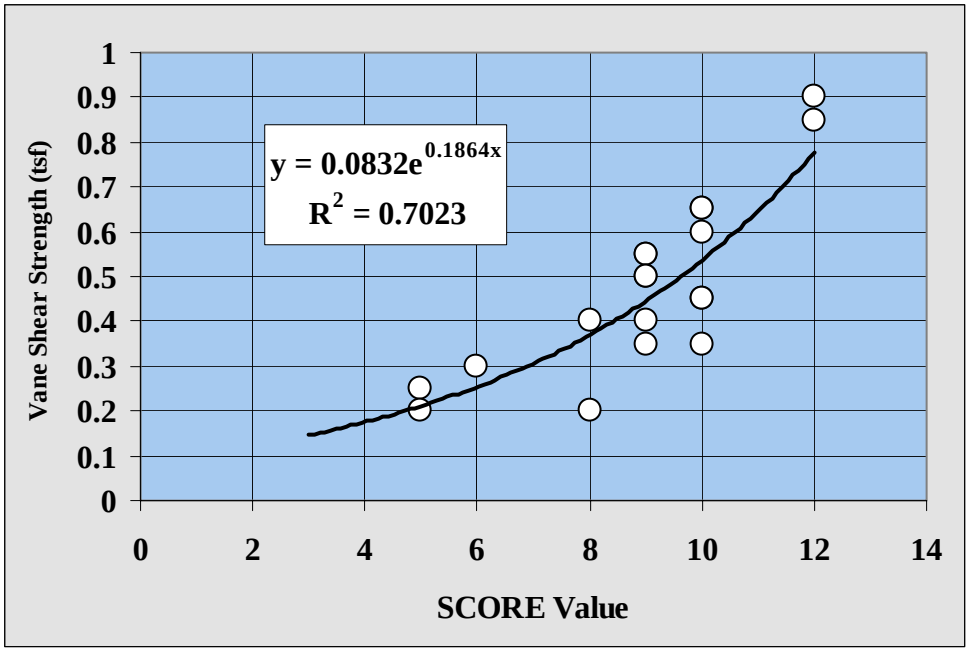

Fig. C3-12. Relationship Between SCORE Values from Soil Consistence Tests and Vane Shear Stress Values Obtained Using a Torvane Instrument

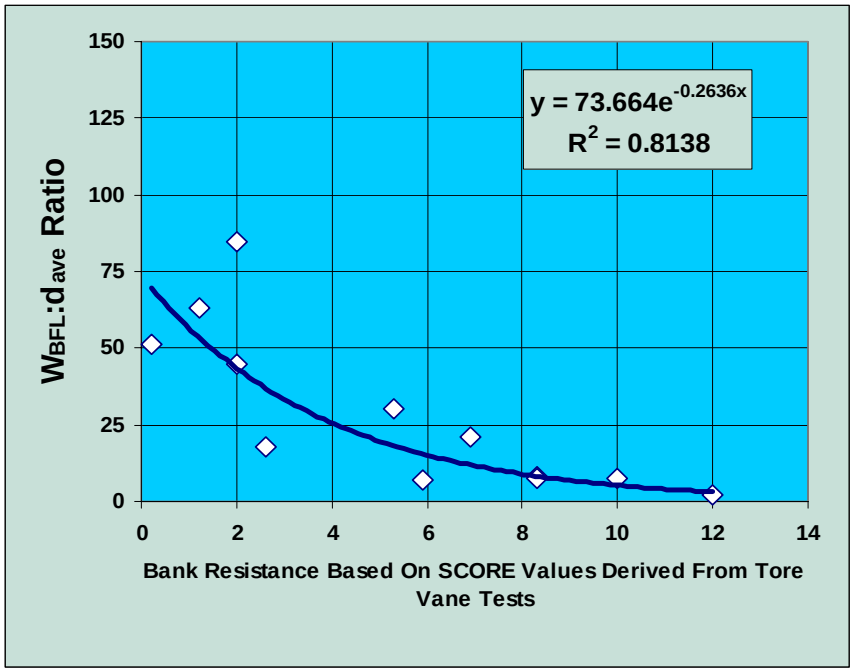

Fig. C3-13. Width/Depth ratios from the Study Sites versus SCORE Values Derived from Vane Shear Strength Measurements

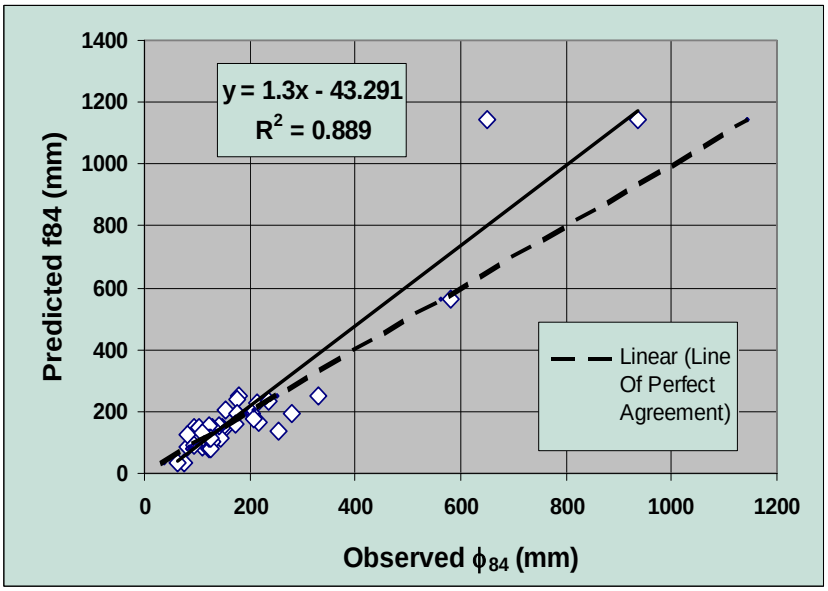

Fig. C3-14. Comparison of measured and predicted sediment sizes (ϕ_{84}) for the Study Sites

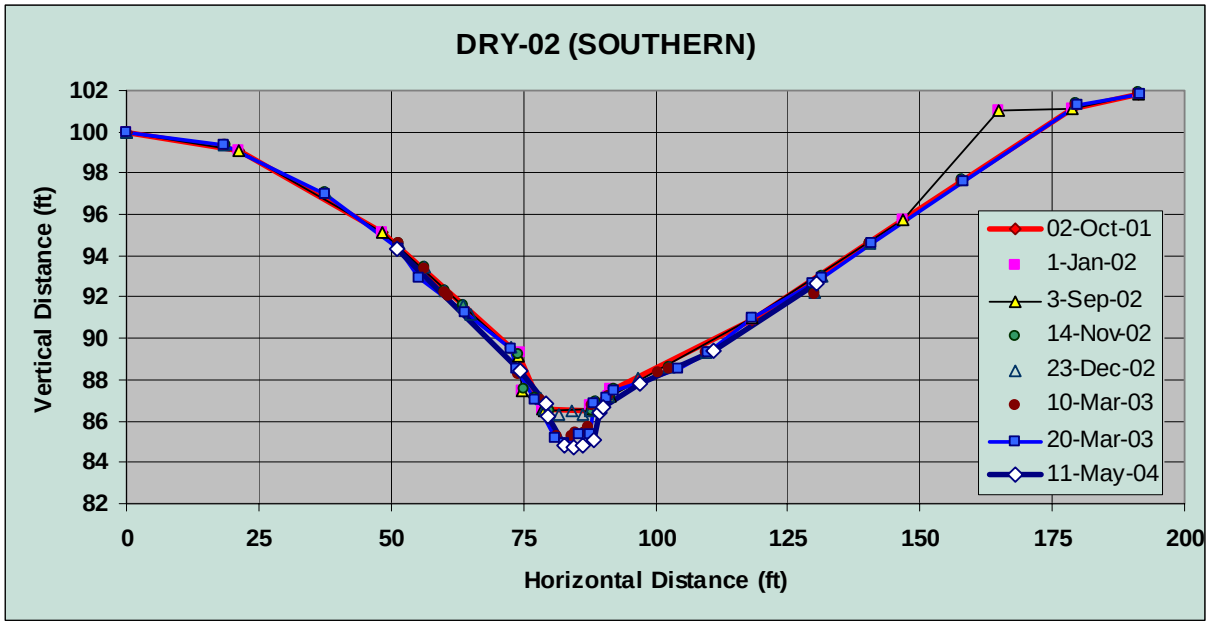

Fig. C3-15. Cross-Section of Dry Creek (2001 through 2004)

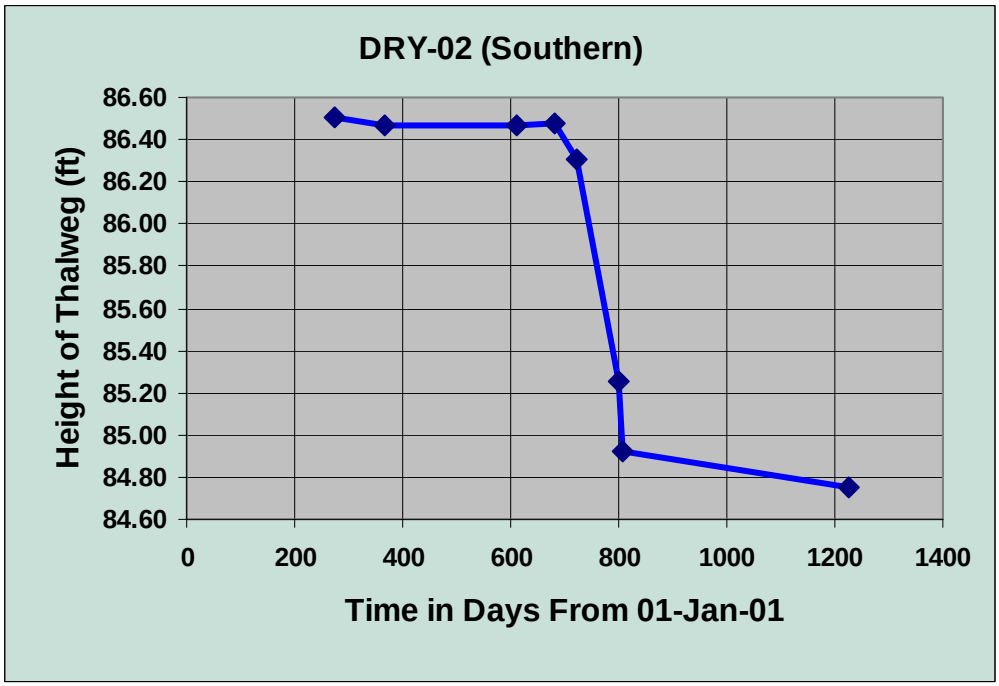

Fig. C3-16. Change in Thalweg Height For Site DRY-02 Between 02-Oct-02 and 11-May-04.

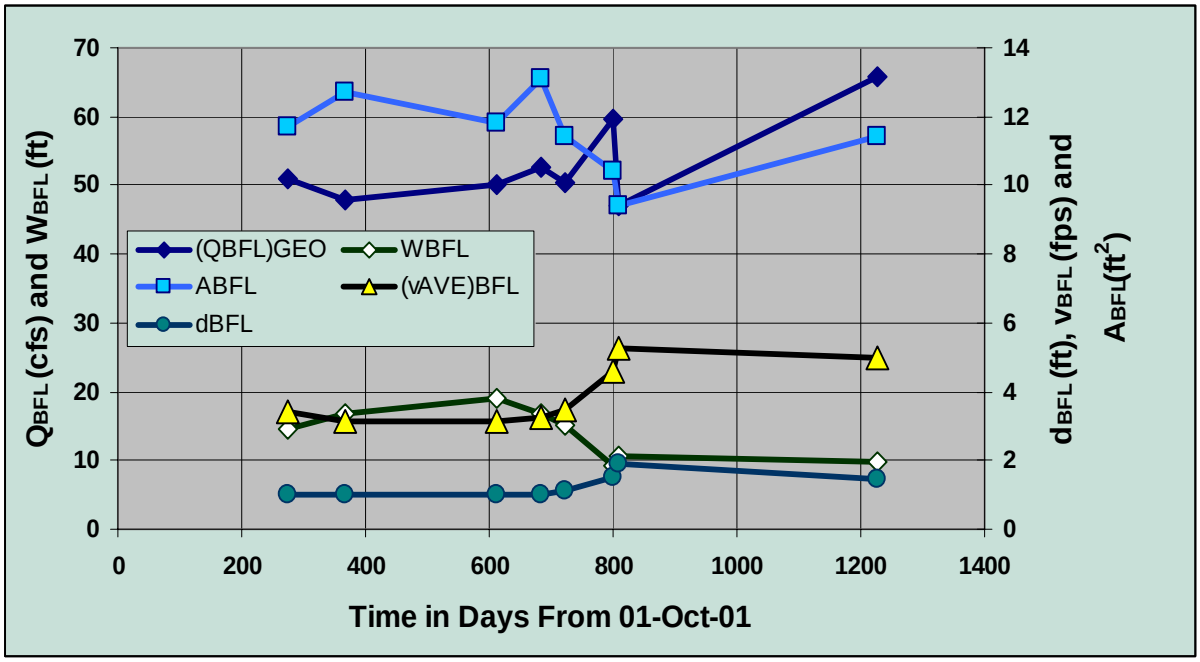

Fig. C3-17. Change in Hydraulic Geometry Parameters Through Time for Site DRY-02.

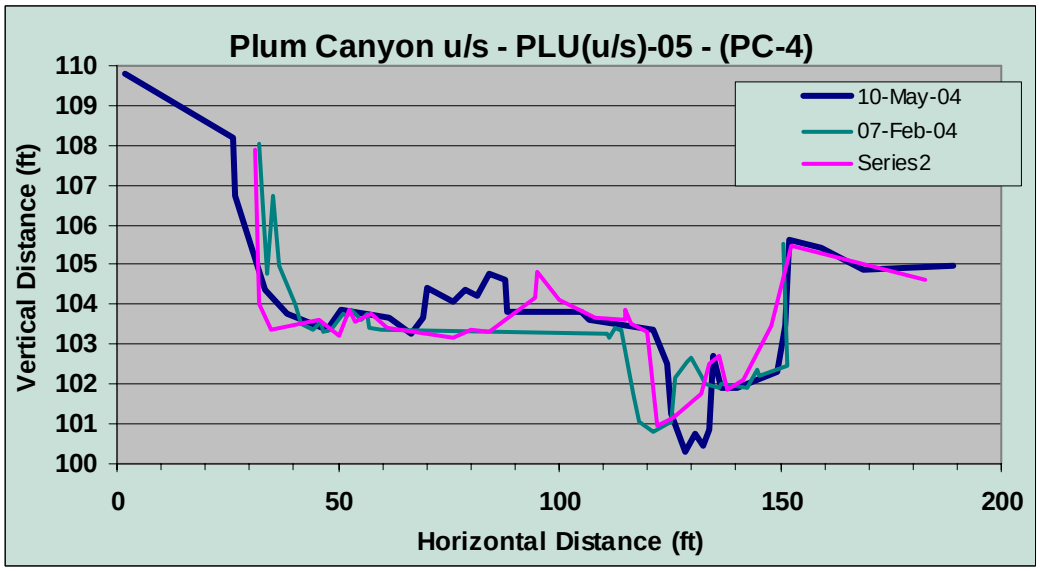

Fig. C3-18. Overlay of Channel Cross-Section Surveys for Site PLU(u/s)-05 in Plum Canyon

C4. Stream Channel Enlargement

C4.1 INTRODUCTION

Previous sections of this Appendix have described the concepts necessary to effectively evaluate channel enlargement, including classification of channels (Appendix C1), the importance of Dominant Discharge (Appendix C2), and the assessment of form and process in natural stream channels (Appendix C3). This section of Appendix C describes the procedure used to evaluate channel changes as well as some very important techniques needed to extend the data set for the historical cases. The procedure to assess the change in channel form associated with land use alteration is based on a comparative approach that is dependent on:

- The availability of historic channel information from which measures of hydraulic geometry and processes of aggradation and degradation can be characterized;
- A basis for standardizing the historic and current estimates of hydraulic geometry parameters for the purpose of comparison; and,
- Correlation of the change in hydraulic geometry parameter values with change in measures of alteration in the sediment and/or flow regime (here after called the "sediment-flow regime").

The procedure results in the estimate of channel cross-section area for a minimum of three conditions:

a) The baseline or pre-development condition;
b) One or more "historical" estimates of channel form (i.e. from a survey taken between the time when baseline condition still existed and the time of the current survey); and,
c) The existing or current land use scenario.

These data are then used to estimate the Enlargement Ratio (R_e) at various points during the process of change, as suggested by the expressions below.

$$(R_e)_{pre} = A_{pre} / A_{pre} \quad [= 1.0] \qquad [C4.1]$$

$$(R_e)_{his} = A_{his} / A_{pre} \quad [1.0 < (R_e)_{his} \leq (R_e)_{ext}] \qquad [C4.2]$$

$$(R_e)_{ext} = A_{ext} / A_{pre} \quad [1.0 < (R_e)_{ext} \leq (R_e)_{ult}] \qquad [C4.3]$$

$$(R_e)_{ult} = A_{ult} / A_{pre} \qquad [C4.4]$$

Where: A = Channel cross section area at the Dominant Discharge stage (ft^2)
"pre" represents the pre-development (or "baseline") case
"his" represents the historic case
"ext" represents the existing case
"ult" represents the ultimate (or fully adjusted) case

As shown in Equation [C4.1] the baseline state represents a boundary condition of zero enlargement producing an Enlargement Ratio of unity (or $(R_e)_{pre} = 1.0$).

The enlargement process may occur over tens of years with the time required to complete the adjustment process a function of the following:

- The stability of the channel system;
- The magnitude of the alteration to the sediment-flow regime;

- The energy of the channel system;
- The resistance of the boundary materials;
- The importance of negative feedback mechanisms; and,
- The size of the watershed.

A conceptual model of the adjustment process for gravel bed channels is provided in Appendix C3 (Section 3-5).

The time required to complete the adjustment process is referred to as the "relaxation period". As a rule of thumb channels exhibiting metastable equilibrium behavior adjust their form within the timeframes presented in Table C4-1.

In accordance with the relaxation period guidelines presented in Table C4-1 it should be noted that the adjustment period for hydraulic geometry parameters or mesoscale fluvial features can be on the order of several decades to over half a century to reach completion. These guidelines were developed from observations obtained on 35 watercourses across North America ranging in watershed area from 0.97 mi^2 to 52 mi^2 with an average value of about 9.5 mi^2. These watersheds are consistent with the spatial scale of the watersheds under investigation in this Study. It is noted however, that among the basins of the larger data set such as the non-study watersheds of Highland Creek (33.1 mi^2), the Rougé River (82 mi^2), the Credit River (316 mi^2) and Onion Creek (350 mi^2) exhibit similar behavior. This suggests that some universality exits in the temporal component of the adjustment process over a wide range in basin size. The sensitivity of the channel to an alteration in the sediment-flow regime is not universal for basins of different CDA sizes. Given the same degree of impact, e.g. a 20% increase in TIMP, channels in smaller watersheds (CDA < 5 mi^2) demonstrate a more rapid and higher degree of enlargement.

The delay between the ultimate enlargement (to the adjusted channel form) and the cessation of the disturbance to the sediment-flow regime complicates the assessment of the impact on channel morphology. For example, a development project within a watershed alters the sediment-flow regime, destabilizes the channel, and initiates a response function as the channel adjusts its form toward a new equilibrium position. A second development project in the same watershed would initiate its own unique response function. If the response function from the first development has not reached maturity, the new response function would be superimposed on the earlier response function. A watershed experiencing multiple development projects throughout the watershed and staggered through time would result in the superimposition of multiple response functions. This scenario applies to Serrano Creek, Borrego Canyon Wash, and Plum Canyon. A single response function applies to Hasley Canyon.

In the cases where a single response function applies, development projects are also relatively small and the lag time (t_l) is only 1.5 to 2.0 years before morphological impacts are observed; these disturbances are considered to be instantaneous. For multiple development projects or phased developments that extend over time periods exceeding the lag time, an area weighted average age of development is computed and used in conjunction with a composite response function.

This Appendix describes the application of a comparative procedure to the Study watercourses. Specifically the following discussion addresses:

a) The quality of the historic channel survey data and the translation of these data into measures of:
   i. Channel hydraulic geometry; and,
   ii. Processes of aggradation and degradation;
b) The use of Dominant Discharge as the basis for standardization of the measures of hydraulic geometry including methods to predict the Dominant Discharge for historic conditions; and,
c) Interpretation of the findings from this assessment and their relevance to stormwater management policy and criteria.

C4.2 THE COMPARATIVE APPROACH

In this approach one needs to superimpose the present cross-section onto historic surveys of channel cross-section form associated with earlier land use conditions. Two aspects of the channel cross-section are of interest:

- The difference in position of the thalweg as determined for the current cross-section survey relative to the historic surveys; and,
- The difference between channel cross-sections for the current and historic surveys for a selected measure of hydraulic geometry.

The positive difference in thalweg elevation may be interpreted as aggradation (an increase in bed elevation through time). Conversely, a negative value may be interpreted as degradation (a decrease in bed elevation through time). These data may be used to determine metrics such as the average, maximum and minimum rates of downcutting in both urbanized and non-urban watercourses.

Cross-section area is the hydraulic geometry parameter typically adopted for the comparative analysis because it accounts for changes in both the width and depth components of cross-section form in a single variable. The cross-section area is measured at the stage of the Dominant Discharge as identified for current and historic land use conditions.

Change in TIMP is commonly adopted as a surrogate for the degree of alteration of the sediment-flow regime associated with urbanization. This is a useful parameter because it is relatively easy to measure and it accounts for the increase in flow rate and volume and the decrease in sediment yield associated with urbanization of a watershed. The hydrologic aspect of TIMP can be illustrated using the peak flow rate of the Rational Formula,

$$Q_p = C_r\, iCDA \qquad [C4.5]$$

Where Q_p = Peak flow rate (cfs)
C_r = f(TIMP) [Rational Formula Runoff Coefficient]
i = rainfall intensity (inches/hour)
CDA = Catchment Drainage Area (acres)

Runoff volume may be estimated using the volumetric runoff equation below (Equation [4.6]).

$$Q_v = C_v\, P_{tot} \qquad [C4.6]$$

Where Q_v = Runoff volume (inches)
C_v = f(TIMP)
P_{tot} = Total event precipitation amount (inches)

While TIMP is relatively easy to determine, the variable has a drawback in that impervious surfaces discharging to pervious surfaces act more like pervious surfaces. Therefore, a more representative variable is FRIMP, the FRaction of IMPervious surface that is directly connected to another impervious surface, such as a storm sewer or to the channel. Unfortunately, FRIMP is more difficult to measure, and it requires field proofing of aerial photographs or topographic maps on a house-by-house basis for representative areas. Transformation functions have been proposed but these equations also require calibration to warrant their application to the study watersheds. However, the level of effort required to

apply FRIMP through direct measurements or using a transformation function is beyond the scope of this study.

While the comparative approach is simple in concept there are a number of logistical and procedural considerations that must be resolved to produce meaningful results. Such considerations include:

a) The need to accurately relocate the position and alignment of the historical surveys;

b) Understanding how representative the historical surveys are in their depiction of the channel form (angle of deflection from normal, number of survey ordinates, location of the survey points. etc.);

c) Insufficient or absent documentation of the longitudinal channel slope, water surface profile or hydraulic grade-line, roughness coefficients, bed material characteristics, presence of Large Woody Debris or other obstructions affecting roughness coefficients and the flow field;

d) Identifying differences in channel features, e.g. pools, steps and riffles and their downstream translocation through the survey transect over the monitoring period;

e) Differences between the historic and current surveys in the resistance of the boundary materials within which the channel is worn;

f) Variations in channel form due to wet and dry years during which the historic and current surveys were recorded;

g) The affect of changes in land use and land use practices, excluding urbanization, on runoff rate and yield during the historic period (e.g. grazing, brush fires);

h) Changes in sediment characteristics, i.e. the physical characteristics of the sediments, the mass of sediment delivered to the system, sediment slugs or waves, bar forms and other factors that may cause aggradation or armoring of the bed and affect channel roughness; and,

i) Differences in anthropogenic influences such as programs to remove large woody debris from within the channel, clear or thin riparian vegetation, establish diversions, create and maintain sediment traps and flood control ponds.

C4.2.1 Data Assessment

Many of the above factors (a through i) were considered and minimized in the selection of the Study Sites. A summary of the assessment of the quality and extent of information available through the historic surveys is provided in Table C4-2. Columns 2, 3 and 11 in Table C4-2 indicate that the data are of high quality with respect to the purposes of this Study, which requires a relatively high resolution of channel features. The exception to the above is the single historical cross-section recorded for Topanga Creek. The exact location and orientation of the historic cross-section could not be reproduced with confidence in the field. Finally the channel detail afforded by the number of survey ordinates recorded was not sufficient for detection of minor changes in cross-section form as required here.

The information required in Columns 4, 5, 7, 8, 9, 10 and 12 were not reported for the historic cross-sections. The data in Columns 4 and 5 are used in conjunction with the cross-section ordinates to solve for Manning's roughness coefficient and subsequently Manning's flow for selected depths of flow. In the absence of these data several estimations and assumptions were made:

- The longitudinal slope is assumed to be the same as the current slope unless there is conclusive geomorphic evidence to the contrary;
- The quantity and physical characteristics of bed materials are assumed identical to the present unless there is geomorphic evidence to the contrary;
- The channel friction factor is determined from the bed materials and the cross-sectional form of the channel; and,

- The Dominant Discharge is estimated as described below.

Columns 7, 8, 9, 10 and 12 in Table C4-2 explain possible departures in channel form from the mean value. This procedure assumes that statistical stationarity in cross-section area applies over the monitoring period (engineering time frame). For example during a wet year scour potential is higher than mean conditions resulting in degradation of the channel bed and reduction in bar forms. In contrast during a dry year the sediment load may exceed channel conveyance capacity resulting in aggradation of the bed. Since the channel will not have had time to adjust the indicators of Dominant Discharge the deeper and more shallow channels in the wet and dry years would result in an over- and under-estimate of the mean value for Dominant Discharge, respectively. Consequently, the estimate of cross-sectional area will result in an over- and under-estimate, respectively in channel enlargement.

It is possible to correct for the over or underestimate of channel cross-section area. Such knowledge would be pertinent in interpreting enlargement relationships for individual watersheds where the number of historic cross-sections are relatively few. However the procedure is complex and beyond the scope of this project. Therefore, in the absence of this information it is assumed that there is no significant departure from the median condition. This source of error diminishes as the number of Sites examined increases. When considered as a whole the database is comprised of 70 historic cross-sections, which is sufficient to average out errors associate with wet-dry year fluctuations in channel morphology.

Column 6 in Table C4-2 addresses the impact of channels as spatially dynamic systems on static or fixed location measurement approaches. The natural (albeit discontinuous) and ongoing translocation of downstream channel features through time may not be amenable to analysis by means of progressive overlays of cross-sections taken at different times at fixed locations along the channel. This concern applies primarily for channels having high geomorphic activity rates and over longer periods, i.e. decades, between successive cross-sections. For example, a long-term observer alongside the channel may see the pool of today transform into a riffle as the features migrate in the downstream direction over the course of one to several decades. The time required for such transitions depends upon the size of the channel system and the rate of downstream translocation of the fluvial features.

The majority of the Study Sites were surveyed beginning in the year 2001 or later (Table C4-3). This produces a monitoring period of less than 3 years for most study sites. The exceptions are Borrego Canyon Wash, Serrano Creek, and Hicks Canyon where historic surveys were taken in 1992 (12 year period), 1991 (13 year monitoring period), and 1986 (18 year monitoring period) respectively,

Fluvial feature separation distances are often measured in an equivalent number of bankfull widths. Using this measure, armored Step-pool channel systems have the shortest separation distances, averaging approximately seven tenths to two times the width of the channel (at the Dominant Discharge stage, or W_{bfl}) between either the pools or the steps. However, the rate of translocation of armored step-pool features is very low, being essentially zero for periods of tens of years followed by significant downstream translocation of material during catastrophic failures under rare flood flow events. The monitoring program began in the year 2000, for duration of less than 4 years, during which time there were no catastrophic events. Consequently, the downstream translocation of fluvial features for watercourses such as Topanga is not an issue.

Unfortunately plan form characteristics were not provided with the historic cross-sections. Consequently, the feature-based method cannot be used without assumptions concerning plan form geometry. Given the advantages and disadvantages of both methods a combined approach was employed using the feature-based method and the direct reproduction of the original cross-section. Fortunately, the cascade-pool and braided channels, which comprised the majority of the channel types examined in this Study did not exhibit large differences in morphology between pool and riffle segments. Therefore, feature-based errors are considered to be minimal.

Another issue is arriving at a common basis for comparison of historic and baseline sites with the current survey data. The method selected for this Study was to determine the cross-section area at the stage of the Dominant Discharge. The Dominant Discharge for current land use conditions was estimated based on bio-geomorphic indicators as described in Appendix C2. However, hydraulic characteristics for the historic and baseline channel conditions must still be established. This leads to the two most important procedural aspect of concern:

- The estimate of the Dominant Discharge for the historic and baseline cross-sections; and,
- The estimate of cross-sectional area for the baseline condition in the absence of survey data.

As alluded to above, there are two conditions that apply which require the use of estimation techniques, and they are the following:

a) The cross-section survey data exist for the historic and baseline conditions but without supporting hydraulic information or identification of the stage of the Dominant Discharge necessitating the estimation of the Dominant Discharge and hence the cross-section area through other means;
b) The cross-section data do not exist requiring estimation of the baseline cross-sectional area through other means.

C4.2.2 Dominant Discharge Estimating Techniques

With reference to a) above in Section C4.2.1 three methods of estimation were employed as follows:

i) The geometry of the channel, e.g. bankfull stage, terraces, tops of bars, etc., was used as a means for determination of the Dominant Discharge;

ii) Hollis (1975) peak flow ratio method; and,

iii) Predictive models (see below) were used to estimate the Dominant Discharge.

The estimates generated from channel geometry were given priority where disagreement between methods occurred. The channel geometry method is described in the following text.

Historic cross-sections with sufficient survey detail allowed for the interpretation of fluvial forms such as terraces and inflection points on the banks. These features were used to identify possible minimum, maximum and average stages for the Dominant Discharge. Estimates of the Dominant Discharge were generated for each stage using Manning's equation as described above. This exercise was repeated for all historic cross-sections at each Site and the resulting estimates of the Dominant Discharge were combined with the current estimate of Dominant Discharge and plotted through time. An example for Dry Canyon is presented in Figure C4-1 for the Dominant Discharge and Figure C4-2 for the associated channel cross-section area. The final estimates for the Dominant Discharge, cross-section area and watershed imperviousness (TIMP) as presented in Figure C4-3.

The data used to create Figure C4-3 are based on historic channel surveys at the Dry Canyon site, with the exception of the data point at time t = 0 days. Although the level of development is very low during the entire period of observation of channel morphology a change in land use was noted between 1998 (TIMP = 0.06%) and 2001 (TIMP = 0.7%, see Table C2-1). Since the historic data did not extend back in time to the 1998 land use condition it was necessary to predict the Dominant Discharge and associated cross-sectional area using other means. Consequently, the first data point in Figure C4-3 was generated using predictive equations developed for this purpose. The development and application of these tools is described in the following sub-section.

With respect to b) in Section C4.2.1 the following approaches were used:

i) Where land use has not changed significantly between the existing or historic survey and the baseline condition then the survey data for the existing or historic survey was used with an

estimate of the Dominant Discharge for the baseline condition to derive a value for the baseline cross-section area. The Dominant Discharge may be estimated using the predictive models described below. The same procedure holds where land use has changed significantly but the time elapsed since the change occurred is within the lag time for channel response.

ii) Where land use has changed significantly or there is reason to believe that the morphology of the existing channel has been altered from the baseline condition then the Relaxation Curve approach was employed.

The relaxation curve approach is a method for extrapolating forward or backward in time knowing the relaxation time (t_r) for the materials within which the channel is worn, the ultimate Enlargement Ratio for the current or historic cross-section $(R_e)_{ult}$ and the lag time (t_l) required before morphological adjustment to a disturbance is manifested through channel adjustment. The Relaxation Curve is of the form,

$$[(R_e)_i - 1] / [(R_e)_{ult} - 1] = m^{*}ln\,[(t_i - t_l) / (t_r - t_l)] + b \qquad [C4.7]$$

The Relaxation Curve for AL-Type channels developed from data collected on watercourses in the Austin, Texas area is illustrated in Figure C4-4.

C4.2.3 Estimates of Dominant Discharge

The preceding approach was applied to the historic data from all Study Sites where there was sufficient detail in the survey data to identify fluvial features. However, this approach could not be applied to all study sites for the following reasons:

a) Some of the Sites lacked the required minimum number of historic surveys;
b) The number of data points used to define the cross-section did not provide sufficient resolution of channel form to permit the definition of fluvial features;
c) The change in channel form was too dynamic and complex;
d) The channel was incised;
e) The materials within which the channel was worn were either too soft or too hard making the identification of Dominant Discharge indicators difficult.

In these situations the estimation of the Dominant Discharge from channel geometry was not sufficiently accurate for the purposes of this Study. To circumvent this problem techniques were developed for the prediction of the Dominant Discharge using bivariate regression models. The predicted values of Dominant Discharge were used with the historic cross-sections to determine the associated cross-section area. This approach was also used to estimate the pre-development or baseline cross-section area where TIMP was known but the cross-section was not surveyed as described below.

Where the value of TIMP was low (TIMP ≤2 %) at the time of the historic survey, the pre-development cross-section area was estimated using the Dominant Discharge predicted for the pre-development land use scenario and the historic cross-section geometry. It is assumed that for low levels of TIMP the change in hydraulic geometry between the pre-disturbance and historic cross-sections may be ignored. For example, in 1998 basin imperviousness for Dry Canyon was estimated to be TIMP = 0.06% but no cross-section was surveyed until 02-Oct-01 (the first historic cross-section). The imperviousness at the time of survey of the historic cross-section was TIMP = 0.7%, for which no significant change in hydraulic geometry was assumed. Consequently, the flow estimated for 1998 land use condition could be applied to the channel geometry surveyed in 2001 to estimate the pre-disturbance cross-section area.

This procedure was also assumed to apply where TIMP > 2% and the time elapsed between the land use change (the time of disturbance) and the time of survey was less than the lag time, the time required for

hydraulic geometry parameters to begin to respond to the alteration in the sediment-flow regime. For a definition of lag time (t_l) see Figure C4-4. The time of disturbance is determined as the area weighted average age of development (Equation [C4.8]). The lag time has been observed to be on the order of one to two years ($1 \leq t_l \leq 2$). Area weighted average age of development is calculated with Equation [C4.8].

$$t_{ave} = (\Sigma\ \Delta DA_i\ TIMP_i\ \Delta t_i) / (CDA\ TIMP_T) \qquad [C4.8]$$

Where t_{ave} = Area weighted average age of development (years)

ΔDA_i = Incremental subarea of basin developed in time period "i" (mi^2)

$TIMP_i$ = Average imperviousness of subarea ΔDA_i (%)

Δt_i = Difference between midpoint of time period "i" and the year of the current channel survey (years)

CDA = Total area of the basin (mi^2)

$TIMP_T$ = Total imperviousness of the basin at time T (%).

Time ranges from 1 year to T years, where year 1 is the baseline land use condition and year T is when the latest channel survey was made. The incremental impervious areas are summed for all of the discrete time periods identified that have associated specific values for developed area and average imperviousness.

In developing predictive models for the Dominant Discharge two methods were considered:

a) The application of USGS flood frequency and magnitude relations; and,

b) The development of a bi-variate model based on CDA and TIMP.

C4.2.4 Regression Analysis

The data in Table C2-1 (see Appendix C2) and Table C4-4 were used to develop relationships between Dominant Discharge (Q_{bfl}), CDA, and TIMP as illustrated in Figures C4-5 and C4-6 respectively.

The assessment of the relationship between Q_{bfl} and TIMP involved removal of four (4) of the ten data points. The rationale for the removal of these points is as follows:

a) Development of a relationship between TIMP and Q_{bfl} required uniformity in CDA size, consequently Topanga Creek (CDA = 18.07 mi^2) and Santiago Creek (CDA = 12.36 mi^2) were removed. The remaining watersheds had drainage areas of 1.22 mi^2 to 2.64 mi^2; and,

b) Infiltration losses through the bed appear to be significant for the downstream sites of Borrego Canyon Wash and Plum Canyon. This is consistent with the physical characteristics of the bed materials (deep loose coarse grained sediments of high porosity). The losses through infiltration produce a significant decrease in the bio-geomorphic estimate of Q_{bfl} relative to upstream Reaches resulting in a negative relationship with CDA. An equation fitted to the data set including these Stations is illustrated in Figure C4-7. The shape of the fitted curve is counter-intuitive to the power function model relating flow rate to CDA. It is argued that these two stations represent a special case due to high infiltration rates. Consequently these two stations were removed from the data set for development of the relationships between Q_{bfl} with CDA and TIMP.

Equations [C4.9] and [C4.10] from Figure C4-5 can be used to provide a first approximation of the Dominant Discharge based on CDA.

$$Q_{bfl} = 57.8\ CDA^{1.16} \qquad (R^2 = 0.809) \qquad [C4.9]$$

and,

$$Q_{bfl} = 448.4\ ln\ (CDA) - 124.5 \qquad (R^2 = 0.893) \qquad [C4.10]$$

Equation [C4.9] is a traditional power function while Equation [C4.10] is a logarithmic transformation. Given the size of the data set it is difficult to justify either function, however non-linear transformations, particularly power functions are typically applied to relationships between flow and Catchment Drainage Area. Of the two functions the logarithmic transformation provides a better fit to the smaller watersheds with the exception of the Borrego Canyon Wash (downstream) and Plum Canyon (downstream) segments. Equation [C4-10], is more representative of the average condition and it has a higer value of R^2, thus it was selected as the preferred univariate model on this basis.

A univariate model based on CDA is not sufficient for prediction of the baseline or historic survey flow rates where urbanization is involved. It is apparent from Figure C4-6, and of no surprise that TIMP has a significant impact on runoff rate for small ephemeral channels in southern California. Bivariate models based on CDA and TIMP have also been developed by the USGS for flood forecasting in urban areas. Consequently, three bivariate models were developed based on CDA and TIMP as presented in Equations [C4.11], [C4.12] and [C4.13]

$$Q_{bfl} = me^{b[\ln(CDA)+c\ln(TIMP)]} \qquad (R^2=0.922) \qquad [C4.11]$$

$$Q_{bfl} = mTIMP^b + k_1CDA^3 + k_2CDA^2 - k_3CDA + k_4 \qquad [C4.12]$$

$$Q_{bfl} = me^{b[\ln(CDA)e^{(cTIMP)}]} \qquad (R^2=0.958) \qquad [C4.13]$$

The relationships for Equations [C4.11] and [C4.13] are presented graphically in Figures C4-7 and C4-8.

Lines of best fit were constructed using plots of predicted versus observed Dominant Discharge (see Figure C4-9 as an example). Predicted versus observed values for Equations [C4.11] through [C4.13] are provided in Table C4-4. Descriptive statistics were also generated for the four models (Table C4-5). From both Table C4-4 and Table C4-5 it can be seen that Equation [C4.13] best reproduces the metric values obtained for the observed data (Q_{bfl} values generated from field estimates of bio-geomorphic indicators). The resulting model provides a good reproduction of the Dominant Discharge as estimated from bio-geomorphic indicators. The model is considered suitable for use in the determination of Dominant Discharge for historic survey data or baseline conditions where resolution of the cross-section form is not sufficient to allow for estimation of Q_{bfl} from the survey data or no survey data are available. Figure C4-9 presents a plot of predicted flow values using Equation [C4.13] as a function of observed Dominant Discharge. The linear regression produced a square of the coefficient of correlation of $R^2 = 0.984$ with the slope of the line approaching unity (m = 1.01) and a y-intercept of b = 24.23. This line closely approximates the line-of-perfect agreement.

While Equation [C4.13] provides a good reproduction of the observed flows there are still discrepancies for specific watersheds. To ensure that the model could be applied to any study site, Equation [C4.13] was calibrated to each watercourse using the following relation:

$$[(Q_{bfl})_{cal}]_i = [(Q_{bfl})_{mod}]_i \times [(Q_{bfl})_{geo} / (Q_{bfl})_{mod}]_{ext} \qquad [C4.14]$$

Where: "cal" stands for the calibrated discharge value for the "i" time marker
"bfl" stands for the Dominant Discharge value

"mod" stands for the model estimated value

"geo" stands for bio-geomorphic referenced value

"ext" stands for values under the existing land use conditions

The calibrated flow values were used to estimate the cross-section areas presented in Table C4-6.

Given the tools described in the preceding Appendices it is now possible to estimate the Enlargement Ratios as determined according to Equations [C4.1] through [C4.4]. The estimates are provided in Table C4-6. In these Tables the column headed "Survey Date" employs two date formats. The day-month-year format indicates that channel cross-section survey data was collected on that day. For Historic Surveys channel geometry was used to estimate the stage of the Dominant Discharge. Using various assumptions as described above the hydraulic characteristics of the channel were determined allowing the construction of a stage-discharge curve and hence an estimate of the Dominant Discharge rate. These estimates of the Dominant Discharge were verified through comparison with model estimates generated using Equation [C4.13]. The channel geometry approach was assumed to be correct if the two estimates were close and considered to be reasonable. Otherwise the model estimate was considered more reliable and used in further calculations. Disparity occurred in cases where the channel geometry was not considered to be of sufficient detail for the purpose defining the stage of the Dominant Discharge. The model estimate of the Dominant Discharge was transposed into a depth of flow and the corresponding cross-section area determined.

For the May 2004 surveys bio-geomorphic indicators identified in the field were used to determine the stage of the Dominant Discharge as described previously. The hydraulic characteristics of the channel were measured or computed as in the case of Manning's 'n' value from which a stage-discharge curve and hence an estimate of the Dominant Discharge rate was obtained. For the pre-development case three different methods were used to determine the Dominant Discharge and associated cross-section area.

Method 1. Where the pre-development channel was surveyed (as denoted by day-month-year format in the "survey date" column of Table C4-6) the approach described above for the historic channel estimates of Dominant Discharge was adopted.

Method 2. Where the pre-development channel was not surveyed the Dominant Discharge was estimated using Equation [C4.13] from land use (TIMP) and watershed (CDA) values. The resulting flow estimates were adjusted using Equation [C4.14] to provide a pseudo-calibration to each study site. The historic cross-section form was assumed to apply to the pre-disturbance condition if the TIMP or lag time criteria apply as described above. In these circumstances only the year is reported in the Survey Date column in Table C4-6.

Method 3. The third approach is based on application of the Relaxation Curves, as illustrated in Figure C4-4 for AL-Type channels. This approach was used as a basis for comparison with the former methods for determining A_{pre}. Secondly, the Relaxation-Enlargement Curve approach is used to predict the ultimate cross-section area due to the enlargement process associated with sediment-flow regime alteration caused by urbanization. The A_{pre} and A_{ult} estimates means that $(R_e)_{ult}$ can be predicted using Equation[C4.4]. The results of the Enlargement-Relaxation Curve analysis are reported in Table C4-7.

Consideration of the undeveloped or baseline study sites indicates that there may be a trend to downcut through time (as discussed in Appendix C3). In addition, Dry Canyon reported a consistent increase in cross-sectional area through the monitoring period of 1993 through 2004 (sections DRY-02, DRY-03 and DRY-04 showed increases in cross-section area [i.e. values of $(R_e)_i$] of 1.19, 1.23, and 1.32 respectively). Topanga Creek also had an increase in channel cross section area from a projected (estimated) baseline condition. However, if only the surveyed measurements of A_{bfl} are used (as opposed to the estimated baseline condition), then the increase was negligible. Four of the five remaining control sections (HAS-04, SAN-01, SAN-02, SAN-03) exhibited a decrease in cross section area [i.e. $(R_e)_i < 1$], and the fifth

(SAN-04) had a slight increase [$(R_e)_i = 1.08$]. In general, the control sections show limited variability about a zero change value of $(R_e)_i$ while progressive lowering of the channel bottom occurred. In contrast, the cross sections at the other (developed) sites consistently had Enlargement Ratio values greater than 1.0, and some that were greater than 2.0 (see SER-03 and SER-05 in Table C4-6).

The estimates of A_{his} and A_{ext} presented in Table C4-7 are also used in the Enlargement-Relaxation Curve assessment approach (as summarized in Table C4-8). The Relaxation Curve is used to go back in time to the pre-development land use condition to obtain an estimate of A_{pre}. The same Curve is also used to forecast to the completion of the enlargement process to provide an estimate of A_{ult}. This is possible using Equation [C4.8] provided the time lapse from the change in land use is known and the Lag Time (t_l) and Relaxation Time (t_r) can be estimated. After the values of A_{ult} for all of the study sites have been estimated, they can be plotted against the corresponding TIMP value for the watershed associated with the site, as shown in Figure C4-10. This figure includes two curves for comparison purposes. The lower curve was derived from data collected over a wide geographical area (Vermont, Texas, Pennsylvania, New York, southern Ontario, British Columbia and Maryland). The upper curve is fitted to the southern California observations of $(R_e)_i$ reported in Table C4-6 for the Enlargement Ratio determined at the time of observation.

Over time (as t_i approaches t_r) the value of the Enlargement Ratio estimated with current surveys will approach the value of the expected, ultimate Enlargement Ratio [i.e. $(R_e)_i \rightarrow (R_e)_{ult}$]. However in the early stages of adjustment (when t_i is smaller than t_r) the estimated Enlargement Ratio [$(R_e)_i$] will be smaller than the ultimate Enlargement Ratio [$(R_e)_{ult}$]. Since the southern California channels are in the early stages of the adjustment process then it is anticipated that the values of the current Enlargement Ratio [$(R_e)_i$] may slightly under estimate the values of the ultimate Enlargement Ratio [$(R_e)_{ult}$].

Table C4-1. Rule of Thumb for Relaxation Time

For streams exhibiting metastable equilibrium behavior.

Boundary Material	Relaxation Time [t_r] (years)	
	Active Channel	Inset Channel
Loose, unconsolidated non-cohesive particles	15-25	30-50
Unconsolidated fine-grained material	35-55	70-110
Unconsolidated but compacted cohesive material	55-65	110-130

Table C4-2. Summary of the Data Coverage and Quality

Summary of the extent of coverage and quality of the historic data for the study sites.

Column 1 Site	Column 2 Relocation	Column 3 Representativenes	Column 4 Slope (S)	Column 5 Bed Material (ϕ_{84})	Column 6 Survey Feature ID	Column 7 Bank Resistance	Column 8 Bed Resistance	Column 9 Wet-Dry Variation	Column 10 Land Use Change	Column 11 Channel Works	Column 12 Sediment Load (Q_s)
Site 1 Topanga	HQ	LQ			LQ					VHQ	
Site 3u Hasley	VHQ	VHQ			VHQ					VHQ	
Site 3d Hasley	VHQ	VHQ			VHQ					VHQ	
Site 4u Plum	VHQ	VHQ			VHQ					VHQ	
Site 4d Plum	VHQ	VHQ			VHQ					VHQ	
Site 7u Borrego	HQ	HQ			VHQ					VHQ	
Site 7d Borrego	HQ	HQ			VHQ					VHQ	
Site 9 Serrano	VHQ	MQ			VHQ					VHQ	
Site 10 Santiago	MQ	HQ			VHQ					MQ	
Site 23 Dry	VHQ	HQ			MQ					LQ	
Site 27 Hicks	HQ	HQ			MQ					VHQ	

VHQ-very high quality, HQ-high quality, MQ-moderate quality, LQ-low quality, VLQ-very low quality or absent

Table C4-3. Data Comparison

Historic survey data timing and correspondence with the May 2004 survey.

Study Site	Section ID: Current Study	Historic Section ID	Date of Survey	Number of Years Prior to 2004
Site 1	TOP-01			
Topanga	TOP-02	TS-1	05-Nov-00	4
			12-May-04	0
	TOP-03			
Site 3u	HAS u/s-04	HC-2	06-Oct-01	3
Hasley upstream			01-Dec-01	3
			14-Dec-02	2
			28-Dec-02	2
			09-May-04	0
Site 3d	HAS d/s-01			
Hasley downstream	HAS d/s-02	HC-2.5	22-Feb-03	1
			14-Mar-03	1
			29-Mar-03	1
			19-Apr-03	1
			09-May-04	0
	HAS d/s-03			
Site 4u	PLU u/s-01			
Plum upstream	PLU u/s-02			
	PLU u/s-03			
	PLU u/s-04	PC-3	13-Oct-01	3
			22-Feb-03	1
			14-Mar-03	1
			29-Mar-03	1
			10-May-04	0
	PLU u/s-05	PC-4	03-Jan-04	0
			07-Feb-04	0
			10-May-04	0
Site 4d	PLU d/s-01			
Plum downstream	PLU d/s-02	PC-1	13-Oct-01	3
			19-Jan-03	1
			22-Feb-03	1
			14-Mar-03	1
			29-Mar-03	1
			10-May-04	0
Site 7u	BOR u/s -01			
Borrego upstream	BOR u/s -02			
	BOR u/s -03	Range 3A	04-Sep-92	12
			01-Apr-93	11
			05-Dec-98	6
			02-Feb-03	1
			06-May-04	0
	BOR u/s-04			
	BOR u/s-05			

Table C4-3. Data Comparison

Historic survey data timing and correspondence with the May 2004 survey.

Study Site	Section ID: Current Study	Historic Section ID	Date of Survey	Number of Years Prior to 2004
Site 7d	BOR d/s-01			
Borrego downstream	BOR d/s-02			
	BOR d/s-03	Range 4D	04-Sep-92	12
			01-Apr-93	11
			02-Feb-03	1
			06-May-04	0
	BOR(d/s)-04			
	BOR(d/s)-05			
Site 9	SER-01			
Serrano	SER-02			
	SER-03	Range D	04-Oct-97	7
			07-May-04	0
	SER-04	Range C	28-Sep-91	13
			01-May-93	1
			07-May-04	0
	SER-05	Range B2	01-Oct-97	7
			07-May-04	0
Site 10	SAN-01	XS-4	28-Apr-95	9
Santiago			13-May-04	0
	SAN-02	XS-3	28-Apr-95	9
			13-May-04	0
	SAN-03	XS-2	28-Apr-95	9
			13-May-04	0
	SAN-04	XS-1	28-Apr-95	9
			13-May-04	0
	SAN-05			
Dry	DRY-01			
	DRY-02	Southern	02-Oct-01	3
			01-Jan-02	2
			03-Sep-02	2
			14-Nov-02	2
			23-Dec-02	2
			10-Mar-03	1
			20-Mar-03	1
			11-May-04	0
	DRY-03	Middle	02-Oct-01	3
			01-Jan-02	2
			02-Sep-02	2
			14-Nov-02	2
			22-Dec-02	2
			10-Mar-03	1
			20-Mar-03	1
			11-May-04	0

Table C4-3. Data Comparison

Historic survey data timing and correspondence with the May 2004 survey.

Study Site	Section ID: Current Study	Historic Section ID	Date of Survey	Number of Years Prior to 2004
	DRY-04	Northern	02-Oct-01	3
			01-Jan-02	2
			02-Sep-02	2
			14-Nov-02	2
			22-Dec-02	2
			10-Mar-03	1
			20-Mar-03	1
			11-May-04	0
	DRY-05			
Site 27	HIC-01			
Hicks	HIC-02	Range A2	05-Sep-86	18
			22-Apr-92	12
			16-Apr-93	11
	HIC-03			
	HIC-04	Range A4	05-Sep-86	18
			22-Apr-92	12
			16-Apr-93	11
	HIC-05			

Table C4-4. Comparison of Flows

Predicted and observed flows from selected multi- and uni-variate models.

	Column1	*Column2*	*Column3*	*Column4*	*Column5*
		Predicted Flow (cfs)			
Study Site	Observed Flow (cfs) $(Q_{bfi})_{ave}$	Model 1: Eqn. [C4.10] $(Q_{bfi})_{ave}$	Model 2: Eqn. [C4.11] $(Q_{bfi})_{ave}$	Model 3: Eqn. [C4.12] $(Q_{bfi})_{ave}$	Model 4: Eqn. [C4.13] $(Q_{bfi})_{ave}$
Topanga Creek	1,427.40	1,639.65	1,719.12	1,979.52	1,394.4
Hasley Canyon u/s	64.80	96.07	69.11	29.86	67.5
Hasley Canyon d/s	73.04	103.76	94.04	70.79	75.5
Plum Canyon u/s	275.61	145.97	197.48	232.26	166.1
Plum Canyon d/s	129.72	74.79	102.56	112.08	91.1
Borrego Canyon Wash u/s	342.51	149.00	214.60	278.34	210.1
Borrego Canyon Wash d/s	247.27	151.92	221.62	199.26	261.5
Serrano Creek	335.34	177.42	270.54	319.36	366.7
Santiago Creek	757.28	1,056.97	605.47	786.52	717.1
Dry Canyon	58.33	72.68	44.43	17.62	50.6
Hicks Canyon	42.94	80.31	56.43	30.68	56.2

Table C4-5. Comparison of Dominant Discharge Statistics

Based on bio-geomorphic indicators, estimates generated using selected multi- and uni-variate models (Borrego d/s and Plum d/s Sites are corrected for bed infiltration losses).

Metric	Observed Flow $(Q_{bfl})_{geo}$	Metric Value By Model			
		Model 1: Eqn. [C4.10]	Model 2: Eqn. [C4.11]	Model 3: Eqn. [C4.12]	Model 4: Eqn. [C4.13]
Mean	341.3	340.8	326.9	368.8	314.3
Standard Error	125.3	155.6	147.2	174.1	123.3
Median	247.3	146.0	197.5	199.3	166.1
Standard Deviation	415.7	516.1	488.2	577.4	408.8
Sample Variance	172,812	266,362	238,343	333,418	167119
Kurtosis	4.73	3.94	8.05	7.08	5.07
Skewness	2.13	2.18	2.76	2.59	2.23
Range	1,384.5	1,567.0	1,674.7	1961.9	1,343.8
Minimum	42.94	72.68	44.43	17.62	50.61
Maximum	1,427	1,640	1,719	1,980	1,394
Sum	3,754	3,749	3,595	4,056	3,457
Count	11	11	11	11	11
Confidence Level (95.0%)	279.3	346.7	328.0	387.9	274.6

Shaded cells indicate best fit to observed value

Table C4-6. Enlargement Data for Study Sites

Site	Cross Sections	Survey Date	TIMP (%)	A_{bfl}	$(R_e)_i$
Site 1	TOP-02 (TS-1)	1949	1.00	138.1	1.00
		1990	2.48	157.9	1.14
		1993	2.62	160.6	1.16
		01-Nov-00	2.82	161.5	1.17
		12-May-04	2.82	162.7	1.18
Site 3u	HAS u/s-04 (HC-2.0)	1990	1.19	15.5	1.00
		1993	1.26	15.5	1.00
		6-Oct-01	1.36	15.5	1.00
		1-Dec-01	1.36	15.7	1.01
		14-Dec-02	1.34	14.5	0.93
		28-Dec-02	1.34	15.8	1.02
		9-May-04	1.34	14.8	0.95
Site 3d	HAS d/s-02 (HC-2.5)	1990	1.19	8.0	1.00
		1-Oct-01	1.34	9.4	1.18
		22-Feb-03	3.27	10.2	1.27
		14-Mar-03	3.27	10.1	1.26
		29-Mar-03	3.27	9.4	1.18
		9-May-04	3.27	9.2	1.15

Table C4-6. Enlargement Data for Study Sites

Site	Cross Sections	Survey Date	TIMP (%)	A_{bfl}	$(R_e)_i$
Site 4u	PLU u/s-04 (PC-3)	2000	0.16	33.0	1.00
		22-Jun-05	1.08	33.7	1.02
		13-Oct-01	1.87	33.7	1.02
		22-Feb-03	1.87	30.0	0.91
		14-Mar-03	5.08	40.0	1.21
		29-Mar-03	21.00		
		10-May-04	21.00	41.9	1.27
Site 4u	PLU u/s-05 (PC-4)	1990	0.15	32.7	1.00
		1993	0.15	32.7	1.00
		2001	0.16	32.7	1.00
		2003	1.73		
		03-Jan-04	16.96	72.7	2.22
		7-Feb-04	16.96	71.4	2.18
		10-May-04	16.96	46.7	1.43
Site 4d	PLU d/s-02 (PC-1)	2000	0.2	19.79	1
		13-Oct-01	1.08	19.79	1.00
		19-Jan-03	1.87	20.31	1.03
		22-Feb-03	1.87	21.29	1.08
		14-Mar-03	5.08	22.56	1.14
		29-Mar-03	21.00	29.97	1.51
		10-May-04	21.00	32.27	1.63
Site 7u	BOR u/s-03 (Range 4A)	1983	1.08	45.0	1.00
		04-Sep-92	1.90	45.6	1.01
		01-Apr-93	5.10	61.5	1.37
		05-Dec-98	5.10	56.1	1.25
		02-Feb-03	21.00	65.9	1.47
		06-May-04	21.00	47.6	1.06
Site 7d	BOR d/s-03 (Range 4D)	1972	1.06	36.0	1.00
		1982	1.06	36.0	1.00
		1990	1.87		
		04-Sep-92	1.87	38.7	1.02
		01-Apr-93	5.08	49.8	1.38
		02-Feb-03	21	58.9	1.64
		05-May-04	21	65.7	1.83
Site 9	SER-03 (Range D)	1949	1.08		
		1982	3.74		
		04-Oct-97	11.18	20.4	1.00
		07-May-04	26.16	55.5	2.71
Site 9	SER-04 (Range C)	1949	1.08		
		1982	3.74	18.9	1.00
		28-Sep-91	5.98	21.5	1.14
		01-May-93	11.18	22.1	1.17
		07-May-04	26.66	37.1	1.97
Site 9	SER-05 (Range B2)	1949	1.08		
		1968	1.14	26.2	1.00

Table C4-6. Enlargement Data for Study Sites

Site	Cross Sections	Survey Date	TIMP (%)	A_{bfl}	$(R_e)_i$
		1982	3.74		
		01-Oct-97	11.18		1.00
		07-May-04	26.66	55.5	2.11
Site 10	SAN-01 (XS-4)	28-Apr-95	0.23	141.6	1.00
		13-May-04	0.24	125.4	0.89
Site 10	SAN-02 (XS-3)	28-Apr-95	0.23	178.4	1.00
		13-May-04	0.24	160.8	0.90
Site 10	SAN-03 (XS-2)	28-Apr-95	0.23	203.0	1.00
		13-May-04	0.24	174.5	0.86
Site 10	SAN-04 (XS-1)	28-Apr-95	0.23	120.6	1.00
		13-May-04	0.24	130.5	1.08
Site 23	DRY-02 (Southern)	1993	0.06	8.7	1.00
		02-Oct-01	0.70	11.3	1.30
		25-Jan-02	0.70	14.2	1.63
		30-Sep-02	0.70	14.9	1.70
		14-Nov-02	0.70	14.4	1.64
		23-Dec-02	0.70	13.5	1.55
		20-Mar-03	0.70	11.1	1.27
		11-May-03	0.70	10.4	1.19
Site 23	Dry-03 (Middle)	1993	0.06	8.7	1.00
		02-Oct-01	0.70	14.1	1.61
		25-Jan-02	0.70	12.8	1.47
		30-Sep-02	0.70	13.2	1.51
		14-Nov-02	0.70	14.6	1.67
		23-Dec-02	0.70	13.2	1.51
		10-Mar-03	0.70	10.7	1.22
		20-Mar-03	0.70	9.4	1.08
		11-May-03	0.70	10.7	1.23
Site 23	Dry-03 (Northern)	1993	0.06	8.7	1.00
		02-Oct-01	0.70	12.0	1.38
		25-Jan-02	0.70	11.4	1.31
		30-Sep-02	0.70	11.6	1.33
		14-Nov-02	0.70	11.3	1.29
		23-Dec-02	0.70	10.9	1.25
		10-Mar-03	0.70	10.8	1.23
		20-Mar-03	0.70	11.2	1.28
		11-May-03	0.70	11.6	1.32
Site 27	HIC-02 (Range A2)	05-Sep-86	0.10	15.5	1.00
		22-Apr-92	0.10	15.5	1.00
		16-Apr-93	1.24	15.5	1.00
		08-May-04	1.24	15.7	1.01

Table C4-6. Enlargement Data for Study Sites

Site	Cross Sections	Survey Date	TIMP (%)	A_{bfl}	$(R_e)_i$
Site 27	HIC-04 (Range A4)	01-Sep-86	0.10	15.5	1.00
		01-Apr-92	0.10	15.5	1.00
		01-Apr-93	1.24	15.5	1.00
		08-May-04	1.24	15.7	1.01

Survey date values that provide only the year indicate that the cross section area (A_{bfl}) and enlargement ratio (R_e) were estimated without surveyed cross sections.

Table C4-7. Summary of Enlargement-Relaxation

Analysis of results from relaxation and enlargement curves for the study sites.

Study Site	A_{pre} (ft^2)	A_{his} (ft^2)	A_{ext} (ft^2)	$(A_{ult})_{ext}$ (ft^2)	$(A_{ult})_{his}$ (ft^2)	TIMP (%)	$[(R_e)_{ult}]_{ext}$	$[(R_e)_{ult}]_{his}$	Ratio of $[(R_e)_{ult}]_{ext}$ to $[(R_e)_{ult}]_{his}$	Predicted $(R_e)_{ult}$ (other source)
TOR-02	155.0	161.5	162.7	174.7	177.8	2.82	1.13	1.15	1.05	1.05
HAS(u/s)-04	15.3	15.5	14.8	15.3	16.2	1.34	1.00	1.06	0.96	0.99
HAS(d/s)-2	7.9	8.0	9.2	10.1	9.1	3.27	1.28	1.15	1.17	1.08
PLU(u/s)-05	32.7	32.7	46.7	92.7	77.6	20.37	2.83	2.37	1.43	2.30
PLU(u/s)-04	33.7	33.7	41.9	74.8	69.2	16.96	2.22	2.05	1.24	1.98
PLU(d/s)-02	19.8	19.8	32.3	46.1	28.7	8.76	2.33	1.45	1.63	1.37
BOR(u/s)-03	40.9	45.6	47.6	91.8	99.7	21.00	2.24	2.44	1.16	2.37
BOR(d/s)-03	34.7	38.7	65.7	126.9	84.5	21.00	3.66	2.44	1.90	2.37
SER-05	26.7	34.6	55.5	107.5	82.7	26.66	4.02	3.10	2.08	3.05
SER-04	19.6	21.5	37.1	72.2	60.7	26.66	3.69	3.10	1.89	3.05
SER-03	26.2	32.1	55.5	79.2	46.6	26.66	3.02	1.78	2.11	3.05
SER-02	23.7	24.7	41.3	59.0	42.1	26.66	2.49	1.78	1.74	3.05
SAN-04	99.2	120.6	130.5	130.6	99.4	0.10	1.32	1.00	1.32	0.93
SAN-03	167.0	203.0	174.5	175.0	167.7	0.10	1.05	1.00	1.05	0.93
SAN-02	146.8	178.4	160.8	161.2	147.4	0.10	1.10	1.00	1.10	0.93
SAN-01	116.5	141.6	125.4	125.7	116.9	0.10	1.08	1.00	1.08	0.93
DRY-04 (No.)	11.7	12.1	14.1	14.1	11.7	0.08	1.21	1.00	1.20	0.93
DRY-03 (Mid.)	13.6	14.1	10.7	10.8	13.7	0.08	0.79	1.00	0.79	0.93
DRY-02 (So.)	14.0	14.5	9.8	10.0	14.4	0.70	0.72	1.03	0.70	0.96
HIC-04	13.6	15.5	8.4	8.8	14.3	1.24	0.64	1.05	0.62	0.98
HIC-02	10.6	12.0	8.9	9.3	11.1	1.24	0.88	1.05	0.84	0.98

Shaded cells indicate data for sites currently in developed watersheds.

Table C4-8. Summary of Dominant Discharge Estimates

Discharge rates under historic land use conditions for specified time markers using Model 4 evaluation procedures.

Watercourse	Dominant Discharge Q_{bfl} (cfs) Using Model 4						$(Q_{bfl})_{geo}$ (cfs)
	1990	1993	2001	2002	2003	2004	2004
Topanga Creek	1,683.53	1,707.00	1,742.16			1,742.2	1,982.8
Hasley Canyon (downstream)	71.70	71.79	71.92	71.89	74.33	74.33	73.04
Hasley Canyon (upstream)	65.57	65.63	65.74	65.71	65.71	66.71	64.8
Plum Canyon (upstream)	101.49	101.34	105.67		105.62	174.51	275.61
Plum Canyon (downstream)	110.83	110.83	115.50		115.45	205.08	129.72
Borrego Canyon Wash (upstream)	107.02	121.29	224.09			224.09	342.51
Borrego Canyon Wash (downstream)	159.61	181.04	405.51			405.51	247.27
Serrano Creek	152.15	186.35	411.99			411.51	335.34
Santiago Creek	847.56	847.56	848.48			849.48	809.65
Dry Canyon	48.20	48.20	48.40			48.4	58.33
Hicks Canyon	53.54	53.54	54.11			54.11	42.94

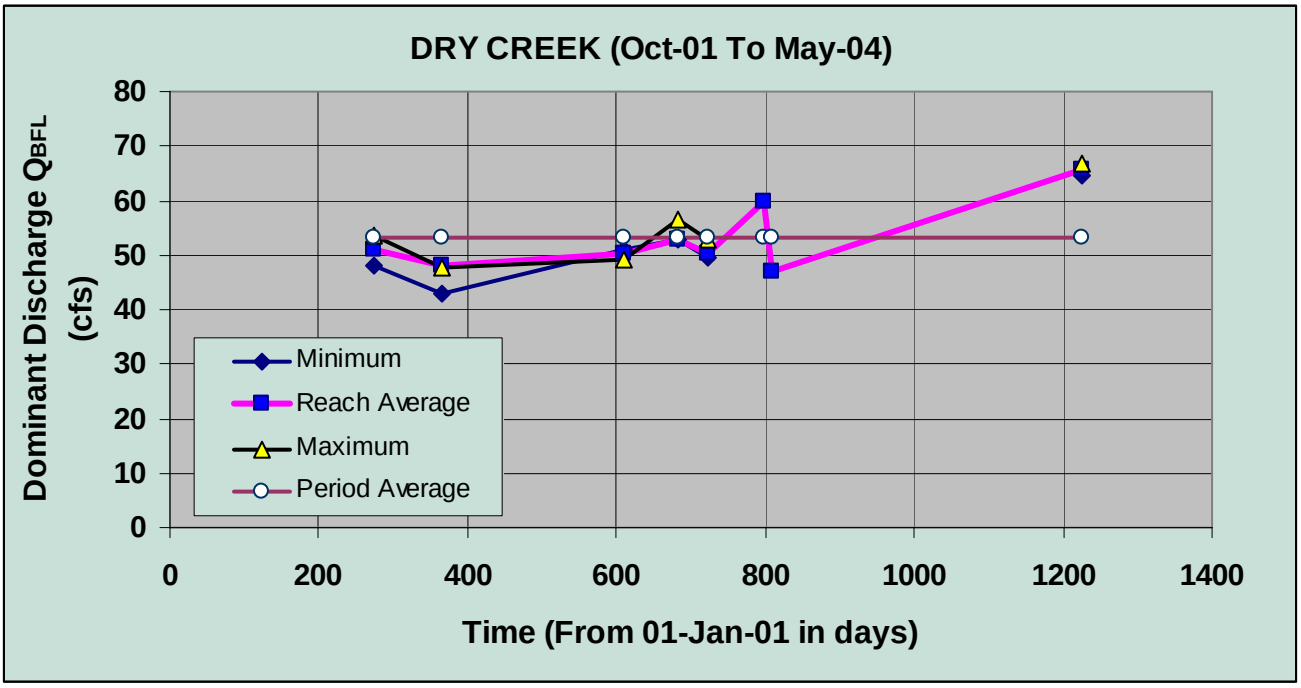

Figure C4-1. Variation in Dominant Discharge Through Time
Based on historic channel geometry data for the Dry Canyon study site.

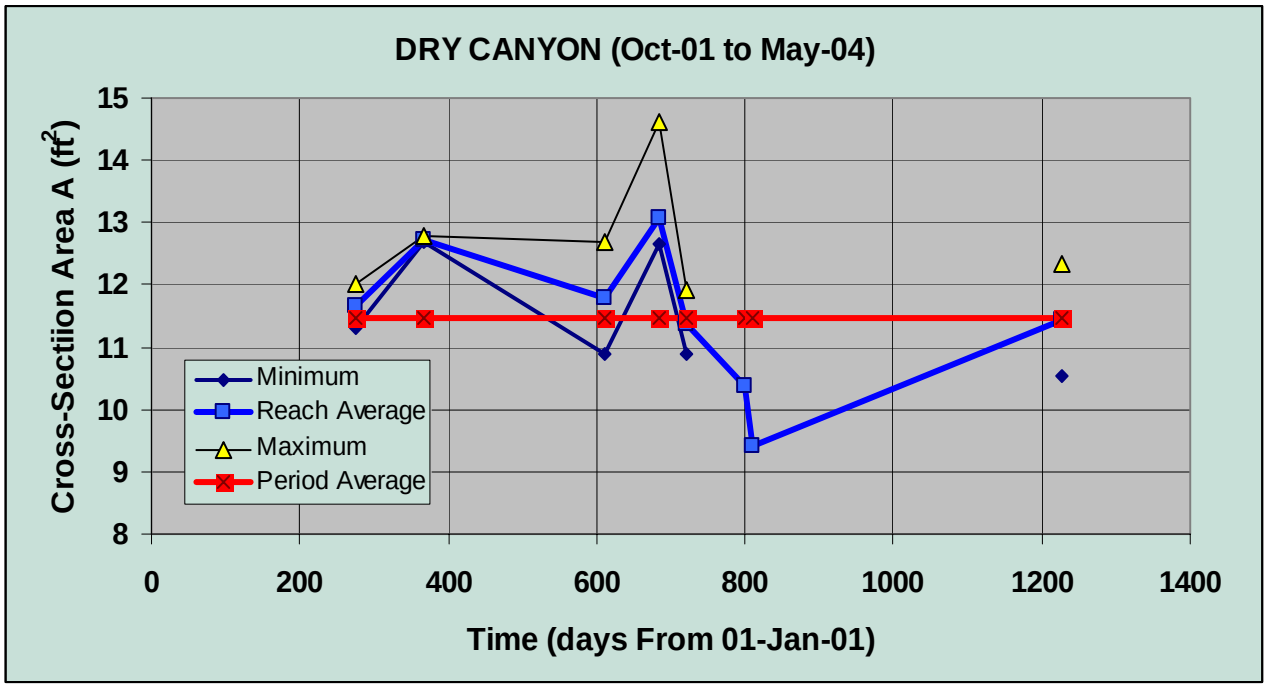

Figure C4-2. Variation Through Time in Estimated Channel Cross-Section Area
Based on Dominant Discharge Values Derived from Historic Channel Geometry.

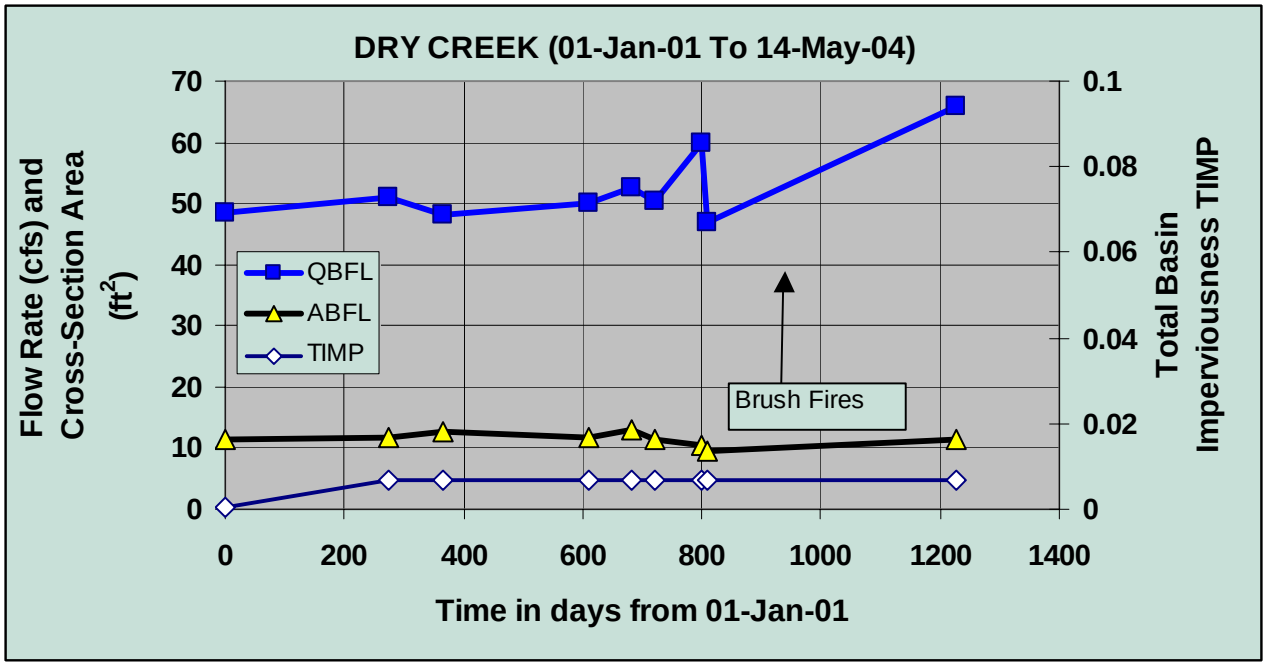

Figure C4-3. Change in Q_{bfl}, Cross-Section Area and TIMP
Data for Dry Canyon study site from January 2001 to May 2004

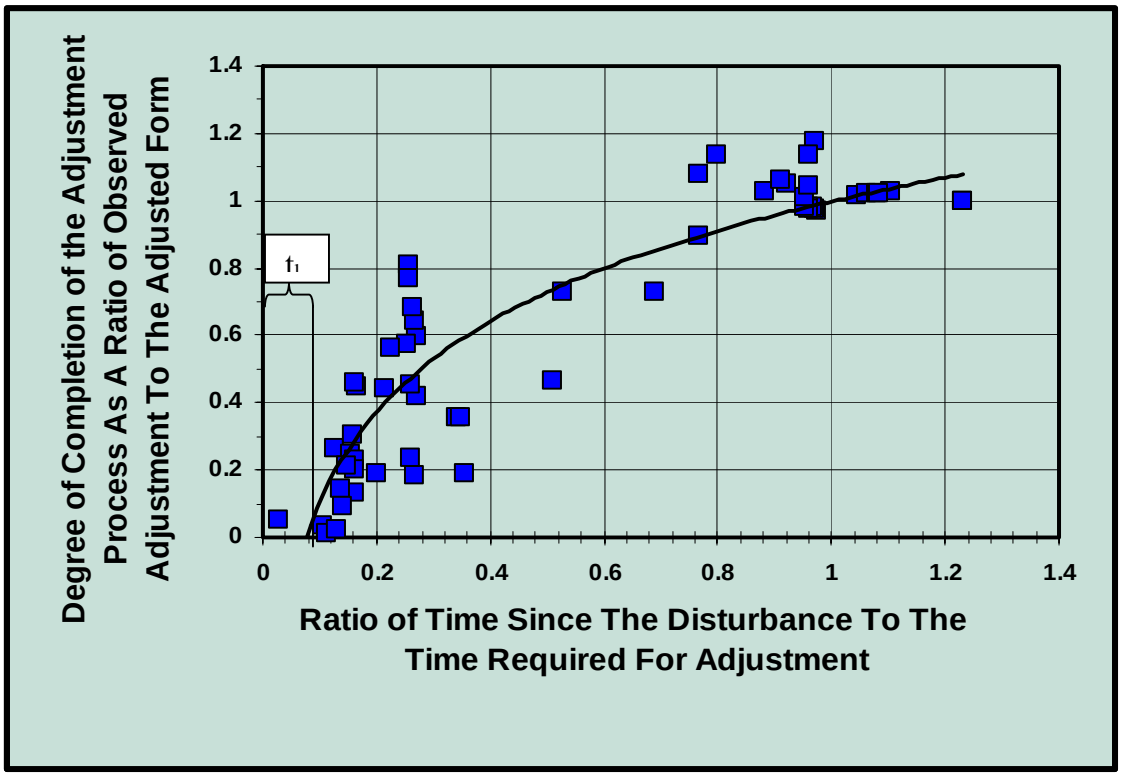

Figure C4-4. Relaxation Curve for AL-Type Channels
Based on Studies of Urban Channels in Austin, Texas.

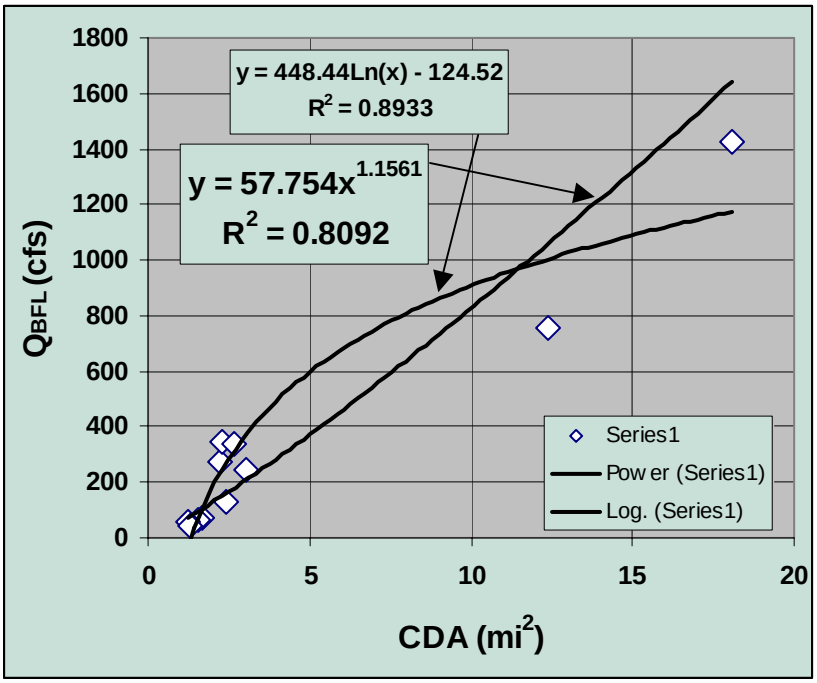

Figure C4-5. Possible Models Based on Catchment Drainage Area
Predicting Dominant Discharge for small ephemeral channels in southern California.

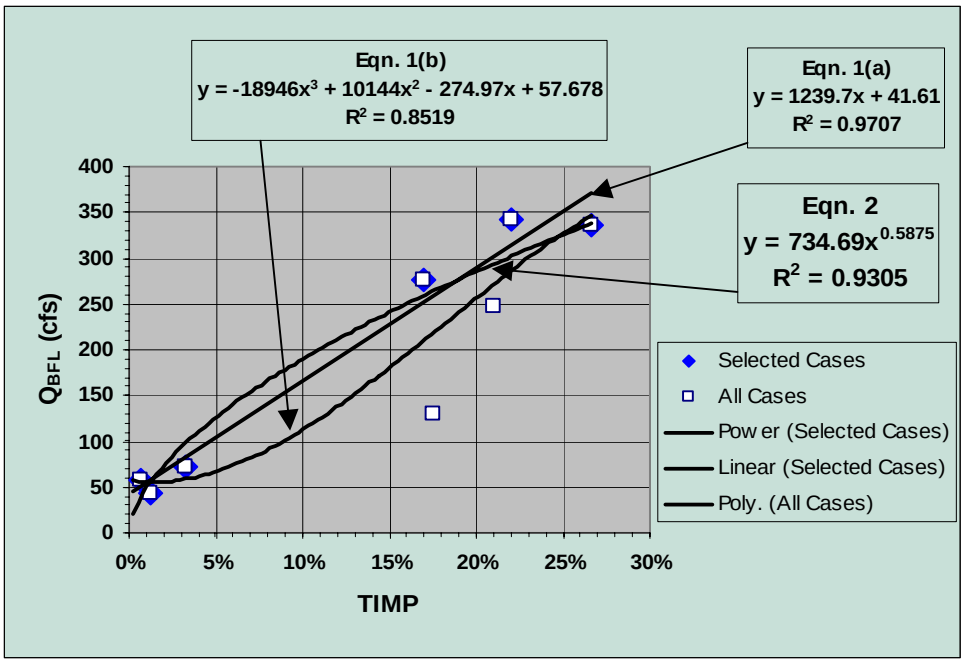

Figure C4-6. Possible TIMP and Q_{bfl} Relationships
Selected ephemeral channels in southern California.

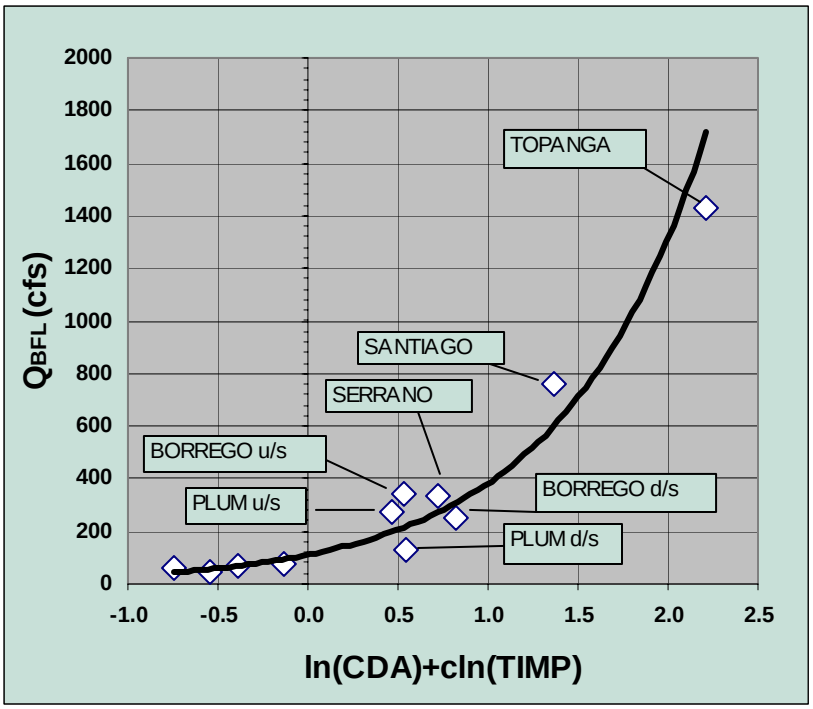

Figure C4-7. Illustration of Fit to Dominant Discharge Values
Estimated from bio-geomorphic indicators using Equation [C4.11]. All stations are included without adjustment for bed infiltration losses.

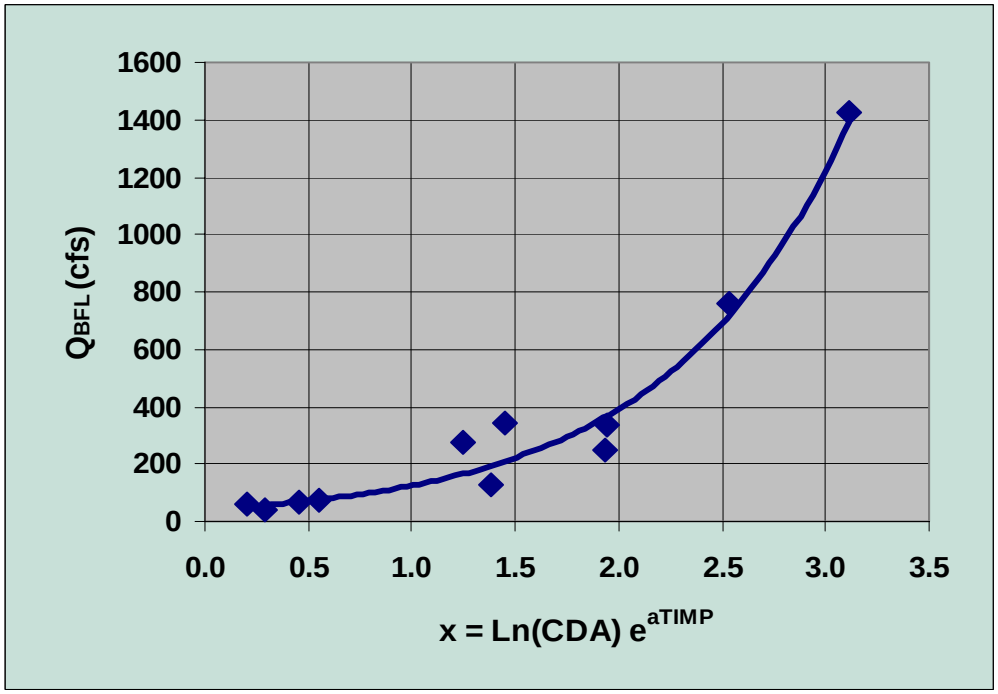

Figure C4-8. Illustration of Fit to Dominant Discharge Values
Estimated from bio-geomorphic indicators using Equation [C4.13]. Data are uncorrected for bed infiltration losses.

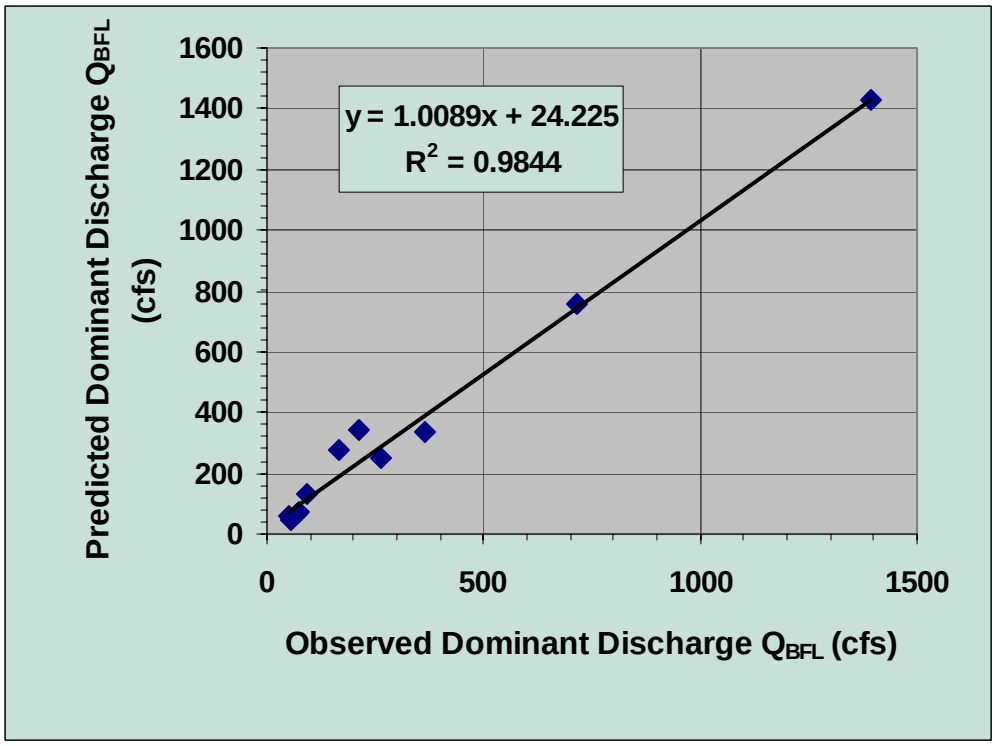

Figure C4-9. Comparison of Predicted Flows to Observed Flows
Flows predicted using Equation [C4.13] with estimated bio-geomorphic field indicators. Borrego d/s & Plum d/s sites have been corrected for bed infiltration losses

.

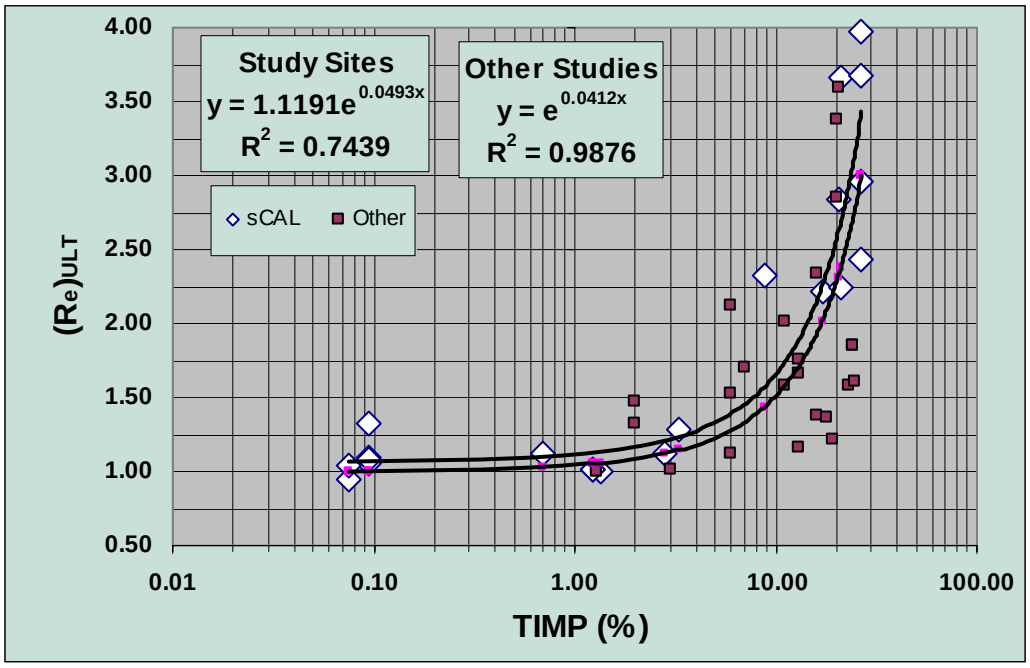

Figure C4-10. Tentative Enlargement Curve
Southern California study sites compared to enlargement data from other geographical areas in Canada and the United States.